Peer-reviewed version available at *Genes* **2020**, *11*, 520; doi:10.3390/genes11050520

Article

Oligodendrocytes remodel the genomic fabrics of functional pathways in astrocytes

Dumitru A Iacobas [1,2,*], Sanda Iacobas [3], Randy F Stout [4] and David C Spray [2,5]

[1] Personalized Genomics Laboratory, Center for Computational Systems Biology, RG Perry College of Engineering, Prairie View A&M University, Prairie View, TX 77446, U.S.A. daiacobas@pvamu.edu
[2] DP Purpura Department of Neuroscience, Albert Einstein College of Medicine, New York, NY 10461, U.S.A.
[3] Department of Pathology, New York Medical College, Valhalla, NY 10595, U.S.A. sandaiacobas@gmail.com
[4] Department of Biomedical Sciences, College of Osteopathic Medicine, New York Institute of Technology, Old Westbury, NY 11568, U.S.A. rstout@nyit.edu
[5] Department of Medicine, Albert Einstein College of Medicine, New York, NY 10461, U.S.A. david.spray@einsteinmed.org

* Correspondence: daiacobas@pvamu.edu; Tel.: +1-936-261-9926

Abstract: We profiled the transcriptomes of primary mouse cortical astrocytes cultured alone or co-cultured with immortalized precursor oligodendrocytes. The experimental set-up (insert systems) prevented formation of gap junction channels but allowed free exchange of the two culture media. The study complements our previously published reports that the genomic fabrics of major functional pathways in oligodendrocytes are substantially remodeled by the proximity of non-touching astrocytes. Here, we present new analysis indicating that the transcriptomic landscape of astrocytes likewise changes significantly in the proximity of non-touching oligodendrocytes. The research was stimulated by the reported transcriptomic similarity between the brains of Cx43KO and Cx32KO mice, both substantially different from that of the Cx36KO mice. Since the three connexins are expressed in different cell types (Cx43 in astrocytes, Cx32 in oligodendrocytes and Cx36 in neurons), altogether these findings support the idea of a "panglial transcriptomic syncytium" in the mouse brain. Going further, our results suggest that integration in a heterocellular tissue modulates not only the expression profile but also the expression control and networking of the genes in each cell phenotype.

Keywords: calcium signaling; chemokine signaling; gap junction; NOD-like receptor signaling; oli-neu cells; pannexin1; PI3K-Akt pathway; thyroid hormone pathway;

1. Introduction

The main glial cells, astrocytes and oligodendrocytes, together with ependymal cells and microglia, form what has been called the "silent majority" of the brain cells. They were considered "silent" because they do not generate action potential as neurons do. Nonetheless, they do signal among themselves by exchanging small (< 1kD) molecules via gap junction channels and release of gliotransmitters that bind the membrane receptors of the cells in the neighborhood. Astrocyte and oligodendrocyte interactions, among themselves and with each other, form the panglial network linking these glial cells throughout the brain. The panglial network provides metabolic support for neuronal activity, thereby impacting both constitutive brain functions such as sleep but also dynamic activities that include learning and cognition [1-3].

Gap junctions provide a two-way route for interaction between oligodendrocytes and astrocytes [4-6], where specific connexin proteins form the intercellular channels in the different cells. Astrocytes express Cx43 (*Gja1*) and Cx30 (*Gjb6*), whereas oligodendrocytes express Cx32 (*Gjb1*) and Cx47 (*Gja12*), and the two cell types communicate through heterotypic connexin pairing. None of these connexins expressed in astrocytes or oligodendrocytes is found in brain neurons (that

express C36 and, to a lesser extent, Cx45). We previously used microarrays to examine gene expression patterns in brains of mice in which genes encoding the astrocyte gap junction protein Cx43, the oligodendrocyte gap junction protein Cx32 or the neuron gap junction protein Cx36 (*Gjd2*) were deleted by homologous recombination [7-11]. These studies revealed that the brain transcriptomes of Cx43KO mice and Cx32KO mice were altered similarly with respect to the wildtype counterpart, whereas they were largely different from those observed in the brain of Cx36KO. Since astrocytes and oligodendrocytes form heterocellularc gap junction channels with each other [12-14], but not with neurons, our results indicated a clear transcriptomic continuity of glial cells. Pan-glial transcriptomic continuity was also confirmed by the disrupted expression of *Gjb1*, the oligodendrocyte coupling partner of the astrocyte *Gjb6* (encoding Cx30) in brains of Cx30 KO mice [15].

Astrocytes and oligodendrocytes very actively modulate the chemical environment of all brain cells. Thus, astrocytes release ATP [16-18] (to mediate Ca^{2+}-signaling among glial cells [19] and in response to sleep-pressure [20]), glutamate to control synaptic strength [21] and several cytokines and chemokines [22-24]. Glial dysfunction is responsible for a wide spectrum of neurological diseases (e.g. [25-8]).

We determined gene expression changes induced in oligodendrocytes co-cultured with but not in contact with astrocytes so as to assure that effects were not mediated by adhesive or gap junctions. That study revealed substantial impact of astrocyte proximity on several functional pathways in oligodendrocytes, with major changes in myelination and its regulation by calcium signaling and cytokine interactions with their receptors [29,30].

In the present study we tested the extent to which the astrocyte-oligodendrocyte interactions are bidirectional by comparing the transcriptomes of mouse cortical astrocytes cultured alone or co-cultured with immortalized precursor oligodendrocytes (Oli neu cells [31]) in insert systems that prevented formation of hetero-cellular gap junction channels [32] but allowed free exchange of the two culture media. Results show that the proximity of oligodendrocytes induced changes in astrocyte transcriptome involving several major functional pathways, including calcium, PI3K-Akt, chemokine, thyroid hormone and NOD-like receptor signaling pathways.

2. Materials and Methods

Cells: Primary cortical astrocytes were isolated as previously described [33] from brains of twelve mouse pups obtained though caesarian section of day 19 pregnant C57Bl/6j female mice. Animals were housed in the Animal Facility of the Albert Einstein College of Medicine and procedures were performed according the IACUC approved procedure (current renewal 20180816, approved 2018). Brains, minced separately in 500µl of 0.05% trypsin-EDTA, were transferred to 1 ml Eppendorf tubes containing 500µl Dulbecco's Modified Eagle medium (DMEM) supplemented with 10% fetal bovine serum, 1% penicillin-streptomycin and spun down at 2000 RPM for 10 min. Cells were resuspended in culture medium, plated in 100 mm culture dishes and maintained in a humidified 5% CO_2 incubator at 37°C. After 1 week in culture, primary confluent astrocytes were trypsinized and re-plated.

The *Oli-neu* cell line, obtained by retroviral transduction of mouse oligodendrocyte precursors with the *t*-neu oncogene [31,34], was generated and kindly provided by Dr. J. Trotter (University of Mainz, Germany). The cells were grown on poly-L-lysine-coated culture dishes in DMEM medium + 1% B27, N2, PSG, SP and 1% horse serum (GIBCO®), maintained at 37°C in 5% CO_2 in a humidified incubator, and passaged following dissociation with Trypsin-EDTA.

Experimental arrangement: The cells were plated as previously described [30] in FalconTM cell

culture 6 well insert systems (www.fishersci.ca), with cortical astrocytes in all plates. *Oli-neu* cells were placed in all the six inserts of the first system and only the culture medium used for *Oli-neu* cells (but without any cells present) in all the six inserts of the second system. Owing to astrocytes adhering to the bottom of the companion plate and *Oli-neu* cells confined to the insert, formation of hetero-cellular gap junction channels between astrocytes and oligodendrocytes [32] was prevented. However, the astrocytes were exposed to the molecules released by the oligodendrocytes diffusing through the 0.4 μm pores of the inserts. The astrocytes were collected in separate labeled Eppendorf vials after 10 days in the Falcon systems. Four vials with well-developed astrocytes were selected from each of the two Falcon systems. Thus, we had four samples (labeled **INS**) with astrocytes co-cultured with *Oli-neu* cells and four samples (labeled **CTR**) with astrocytes in *Oli-neu* culture medium alone.

Microarray: Total RNA was extracted as previously described [35] with Qiagen RNeasy minikits separately from each of the eight selected vials from the two Falcon systems. RNA concentration before and after reverse transcription in the presence of Cy3/Cy5 dUTP was determined with NanoDrop ND 2000 Spectrophotometer and quality with Agilent RNA 6000 Nano kit in an Agilent 2100 Bioanalyzer. 825ng of differently (Cy3/Cy5) labeled biological replicas were hybridized 17h at 65°C with Agilent G2519F unrestricted AMADID Release GE 4x44k 60mer two-color mouse gene expression microarrays using the "multiple yellow" strategy. The chip (4 microarrays) was scanned with an Agilent G2539A dual laser scanner at 5μm resolution in 20-bit scan mode (>10^5 dynamic range) and primary analysis performed with (Agilent) Feature Extraction 11.6 software.

All corrupted spots or with foreground fluorescence less than twice background fluorescence in any of the eight samples were eliminated from the analysis. Data were normalized using our standard algorithm alternating intra- and inter-array normalization to the median of the background-subtracted fluorescence. Spots probing the same transcript were grouped into redundancy groups. Agilent mouse 4x44k microarrays used in this study hybridizes 30,175 distinct transcripts, out of which 22,657 are probed by single spots. The largest redundancy groups (13 spots) probed the genes: *Abcc5* (ATP-binding cassette, sub-family C (CFTR/MRP), member 5), *Cpne4* (copine IV), *Csf1* (estrogen receptor 1 colony stimulating factor 1), *Esr1* (estrogen receptor 1), *Mapk1* (mitogen-activated protein kinase 1), *Oprm1* (opioid receptor, mu 1), *P2rx3* (purinergic receptor P2X, ligand-gated ion channel, 3) and *Socs2* (suppressor of cytokine signaling 2).

Data Analysis: Profiling four biological replicas of each condition produces with adequate statistical power three independent measures for each transcript: i) average expression level, ii) variability of transcript abundance and iii) expression coordination with each other transcript [36]. The rarely used analysis of expression variability provides information about the degree to which homeostatic mechanisms limit range of transcript abundance and the analysis of expression coordination allows assessment of interactions within gene networks that underlie functional pathways. We report here the astrocyte genes that were up-or down-regulated, exhibited stricter or looser expression control and were differently networked when the oligodendrocytes are close by. The medians of the three independent gene features can be used to characterize selected groups of genes and transcriptomic networks associated to functional pathways.

Pathway analysis: Kyoto Encyclopedia for Genes and Genomes [37,38] was used to select the genes responsible for calcium (map mmu04020), PI3K-Akt (mmu04151), chemokine (mmu040602), thyroid hormone (mmu04919) and NOD-like receptor (mmu04621) signaling pathways. We have also studied the remodeling of the actin cytoskeleton (mmu04810), autophagy (mmu04140), cell-cycle (mmu04110), circadian rhythm (mmu4710) and gap junction (mmu04540). Particular attention was given to the regulation of the astrocytic receptors involved in modulating the activity of the glutamatergic (mmu04724), GABAergic (mmu04727), cholinergic (mmu04725), dopaminergic (mmu04728) and serotonergic (mmu04726) interneuron synapses.

These pathways were selected for the following reasons:

- Calcium signaling (hereafter denoted by **CAS)** is evolutionary the oldest, yet most common way by which a wide diversity of cells communicates to each other [19]. Change in calcium signaling is a major modulator of the glia cell behavior [39].

- PI3K-Akt signaling (hereafter denoted by **PA**) is pivotal for the growth, metabolism, survival, angiogenesis, autophagy, and chemotherapy resistance of the malignant astrocytic glioma [40].

- Chemokine signaling (**CS**) between astrocytes and oligodendrocytes, most likely the main crosstalk in our experiment, is important for glial development and stimulating regeneration and repair [41].

- The thyroid hormone signaling pathway (**TH**) was chosen because astrocytes are thought to be the main regulator of thyroid hormone in the brain and T3 is a main driver of oligodendrocyte maturation [42, 43].

- NOD-like receptor signaling pathway (**NOD**) was chosen because of its role in cognition, anxiety and activation of the hypothalamic-pituitary-adrenal axis [44].

- The actin cytoskeleton (**AC**), is an elaborate cytoplasmic protein structure central in determining cell and organ size and morphology, intracellular transport and cell division [45].

- Autophagy (**AU**) is a major degradation pathway, essential in maintaining astrocyte function [46]

- Cell-cycle (**CC**) is expected to be one of the most dependent pathway on the cellular environment.

- The circadian rhythm (**CR**) – increasing evidence indicates that astrocytes are very important players in the regulation of circadian rhythms [47].

- Even though the experimental set up did not allow formation of hetero-cellular gap junction channels, the very proximity of the oligodendrocytes might have an effect on the expression level and networking of the gap junction (**GJ**) pathway in astrocytes.

Relative Expression Variability: Expression variability is normally quantified by the coefficient of variation (CV). However, owing to the non-uniform redundancy of the microarray spots probing the same transcript), we use a Bonferroni-like corrected p-val < 0.05 significant chi-square mid-interval estimate of CV for each distinct transcript in each condition which we term Relative Expression Variability (REV) [36]:

$$REV_i^{(condition)} = \underbrace{\frac{1}{2}\left(\sqrt{\frac{r_i}{\chi^2\left(r_i;0.975\right)}}+\sqrt{\frac{r_i}{\chi^2\left(r_i;0.025\right)}}\right)}_{\text{correction coefficient}}\sqrt{\underbrace{\frac{1}{R_i}\sum_{k=1}^{R_i}\left(\frac{s_{ik}^{(condition)}}{\mu_{ik}^{(condition)}}\right)^2}_{\text{pooled CV}}}\times 100\%$$

μ_{ik} = average expression level of gene i probed by spot k (= 1, ..., R_i) in the 4 biological replicas
s_{ik} = standard deviation of the expression level of gene i probed by spot k
$r_i = 4R_i - 1 =$ number of degrees of freedom
R_i = number of microarray spots probing redundantly gene *i* (1)

Expression regulation: A gene was considered to be significantly regulated if its absolute fold-change $|x|$ exceeded the corresponding individual gene cut-off (*CUT*) that considers the combined contributions of the biological variability among biological replicas and the technical noise in achieving the measurement. This method eliminates most of the false positive and negative hits that result from an arbitrary fixed cut-off (such as 1.5x) [48].

$$|x_i| > CUT_i = 1+\frac{1}{100}\sqrt{2\left(\left(REV_i^{(INS)}\right)^2+\left(REV_i^{(CTR)}\right)^2\right)} \quad , \quad where:$$

$$x_i = \begin{cases} \dfrac{\mu_i^{(INS)}}{\mu_i^{(CTR)}} & , \text{ if } \mu_i^{(INS)} > \mu_i^{(CTR)} \\ -\dfrac{\mu_i^{(CTR)}}{\mu_i^{(INS)}} & , \text{ if } \mu_i^{(INS)} < \mu_i^{(CTR)} \end{cases} \quad (2)$$

Pathway regulation: The regulation of a given pathway was analyzed from the perspective of both percent of genes that were significantly regulated (using the above criterion of the absolute individual gene fold-change cut-off) and the Weighted Pathway Regulation [36]:

$$WPR(\Gamma) = \left\langle \mu_i^{(CTR)} \times \left(|x_i|-1\right)\times\left(1-p_i\right)\right\rangle_{i\in\Gamma} \times 100 \quad (3)$$

In (3), p_i is the p-value of the heteroscedastic (two tails, unequal variance) *t*-test of the means equality in the two conditions.

WPR quantifies the contributions of the composing genes to the pathway alteration by considering their normal expression levels (here in CTR), their absolute departure from the equal expressions in both conditions and the statistical significance of their regulation.

Expression correlation: Pair-wise Pearson product-moment correlation analysis of the ($\log_2$) expression levels across the biological replicas was performed to identify the significantly (p-val < 0.05) synergistically, antagonistically and independently expressed gene pairs in each condition. Two genes were considered as ($p < 0.05$) significantly synergistically expressed ($\varrho > 0.95$) when their expression levels are positively correlated across biological replicates, while they are antagonistically expressed ($\varrho < -0.95$) when their expression levels manifest opposite tendencies. The genes are considered as independently expressed when ($|\varrho| < 0.05$). The statistical significance of the correlation coefficient was determined with the two-tail *t*-test for the degrees of freedom df = 4(biological replicas)*R (number of spots probing redundantly each of the correlated transcripts) – 2. [49]. The correlation analysis was used to determine the remodeling of gene networks.

Gene Commanding Height: The Gene Commanding Height (GCH) score was introduced recently [50,51] to establish the gene hierarchy in each condition. It combines an estimate of the transcription control of that gene with a measure of its expression coordination with each other gene:

$$GCH_i^{(condition)} = \underbrace{\frac{\left\langle REV^{(condition)} \right\rangle}{REV_i^{(condition)}}}_{\text{transcription control estimate}} \times \underbrace{\exp\left(4\left(\overline{\rho_{ij}^{(condition)}} \right)^2 \Big|_{\forall j \neq i} \right)}_{\text{measure of expression coordination}}, \quad where: \tag{4}$$

$\left\langle REV^{(condition)} \right\rangle$ = median of all genes REVs in "condition" CTR or INS

$\rho_{ij}^{(condition)}$ = Pearson correlation coefficient of genes i and j $\log_2$ expression levels

The top gene (highest GCH) was termed the Gene Master Regulator and is expected to be the most influential for the preservation of the cell phenotype,

3. Results

3.1. Overview

Raw and processed gene expression data were deposited in the publicly available website https://www.ncbi.nlm.nih.gov/geo/query/acc.cgi?acc=GSE109035. In total, 18,891 unigenes were adequately quantified in all 8 samples, out of which almost 20% were significantly regulated in astrocytes cultured in the proximity of oligodendrocytes (INS) compared to astrocytes cultured alone (CTR).

The analyzed pathways were composed of the following numbers of unigenes: **AC** = actin-cytoskeleton (181 unigenes), **AU** = autophagy (122), **CAS** = calcium signaling (137), **CC** =cell cycle (116), **CR** = circadian rhythm (29), **CS** = chemokine signaling (139), **GJ** = gap junction (78), **NOD** = NOD-like receptor signaling (143), **PA** = PI3K-Akt signaling (294), **TH** = thyroid hormone signaling (106). In addition to these pathways, we have considered also a group of 22 astrocyte genes, termed **sy**napse **r**egulators (**SYR**), that modulate the synaptic transmission between neurons in the brain.

An overview of the microarray results is presented in Figure 1. Thus, Figure 1(a) shows the alterations of the expression level, Figure 1(b) the alterations of Relative Expression Variability (REV) and Figure 1(c) the changes in the Gene Commanding Height (GCH) for all quantified unigenes (ALL) and each of the selected functional pathways. In addition, Figure 1(d) presents the GCH scores of the top 5 genes in each condition and the corresponding GCH in the other condition.

Alterations of the expression level are presented as percentages of the up- and down-regulated genes, and as the Weighted Pathway Regulation (WPR). The individual gene cut-off (*CUT*) ranged from 1.06x for TGF-beta activated kinase 1/MAP3K7 binding protein 1 (*Tab1*) from NOD, up-regulated by 1.25x, to 3.61x for guanylate cyclase 1, soluble, alpha 2 (*Gucy1a2*) from GJ, significantly upregulated by 35.94x. Using the uniform 1.5x absolute fold-change would result in 4% false hits and neglect 6% significant regulations as a consequence of sample variability.

Table S1 in the Appendix lists the genes whose >1.5x absolute fold-change did not meet the individual CUT criterion ("false hits" for the uniform 1.5x fold-change cut-off). Tables S2 and S3 in the Appendix list the genes considered as significantly up- and down-regulated according to our criterion, although for some of them was below the 1.5x traditionally used as a cut-off.

For the entire transcriptome, the percentage of down-regulated genes is balanced by that of the up-regulated (9.63% down- vs. 9.89% up-regulated, down/up ratio = 0.97). However, the

percentages of the down- and up-regulated genes are quite dissimilar tor individual pathways, the most notable example being the cell cycle pathway where the ratio of down to up regulated genes is 31x. The bias indicates that oligodendrocyte proximity had a profound inhibitory effect on this pathway in astrocytes.

Note in Fig. 1(b) that REV was higher in co-cultured astrocytes for all gene groups except those encoding the CS and GJ pathways and was statistically significant for ALL, AC, AU, CAS, PA and TH groups. Figure 1(c) indicates statistically significantly higher median GCH of the synaptic receptors, gap junction, autophagy and chemokine signaling. GCH values were significantly lower for the circadian rhythm pathways, while the differences of the other pathways were not statistically significant.

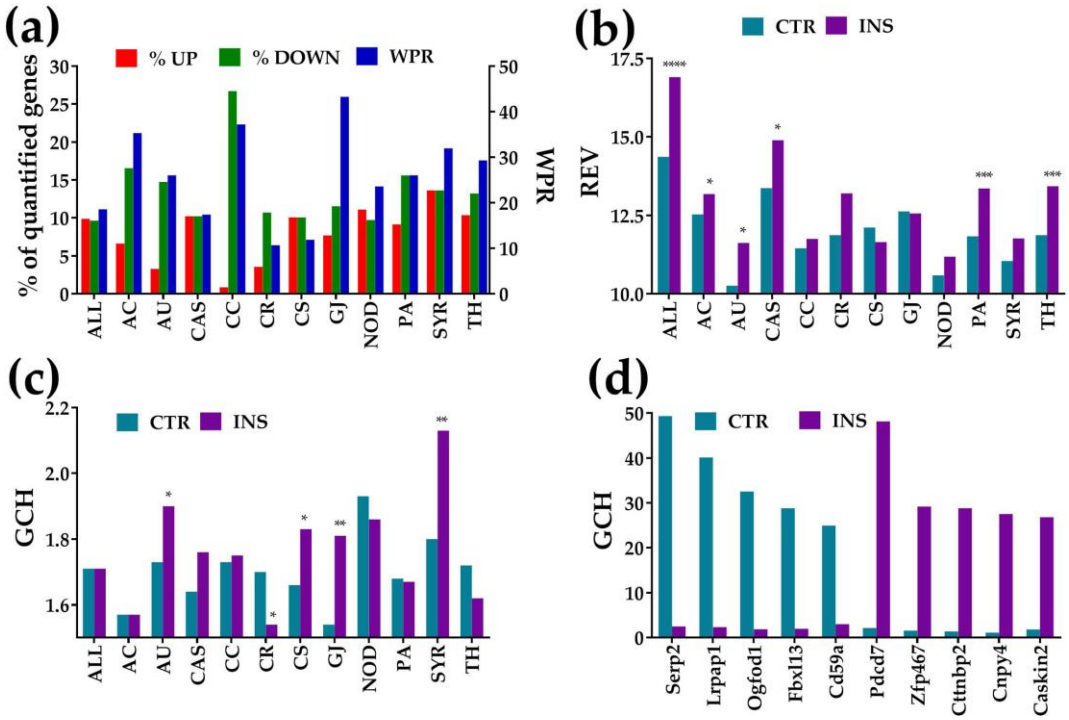

Figure 1. Alterations of the expression level, expression variability and gene commanding height for all 18,891 quantified unigenes (ALL) and selected functional pathways and individual genes. **(a)** Percentages of significantly up/down regulated genes and the Weighted Pathway Regulation (WPR) score of the selected pathways in astrocyte co-cultured with *Oli neu* cells (INS) with respect to astrocytes cultured alone (CTR). **(b)** Median Relative Expression Variability (REV) of selected gene groups in each condition. **(c)** Median Gene Commanding Height (GCH) of selected gene groups in each condition. **(d)** Top 5 genes (highest GCH scores) in each condition and their GCHs in the other condition. Statistical significance: * $p < 0.05$, ** $p < 0.01$, *** $p < 0.005$, **** $p < 0.0001$.

The gene with the highest GCH in the CTR astrocytes was *Serp2* (stress-associated endoplasmic reticulum protein family member 2) with GCH = 49.31 (GCH = 2.49 in INS astrocytes), while in the INS astrocytes it was *Pdcd7* (programmed cell death 7), with GCH = 48.13 (compared to GCH = 2.14 in CTR astrocytes).

3.2. Regulation of gap junction, cell-cycle, actin-cytoskeleton and circadian rhythm pathways

Figures 2 and 3 show the regulation of the KEGG-determined gap junction and cell-cycle pathways, and Figures S1 and S2 in the Appendix the regulation of the actin-skeleton and circadian

rhythm pathways. Graphs below pathways present the expression ratios (together with the respective individual gene fold-change cut-offs, both negative for down-regulation) of significantly altered genes. Each figure also shows the GCH scores of the pathway genes in the two conditions.

3.2.1. Significantly regulated gap junction-associated genes

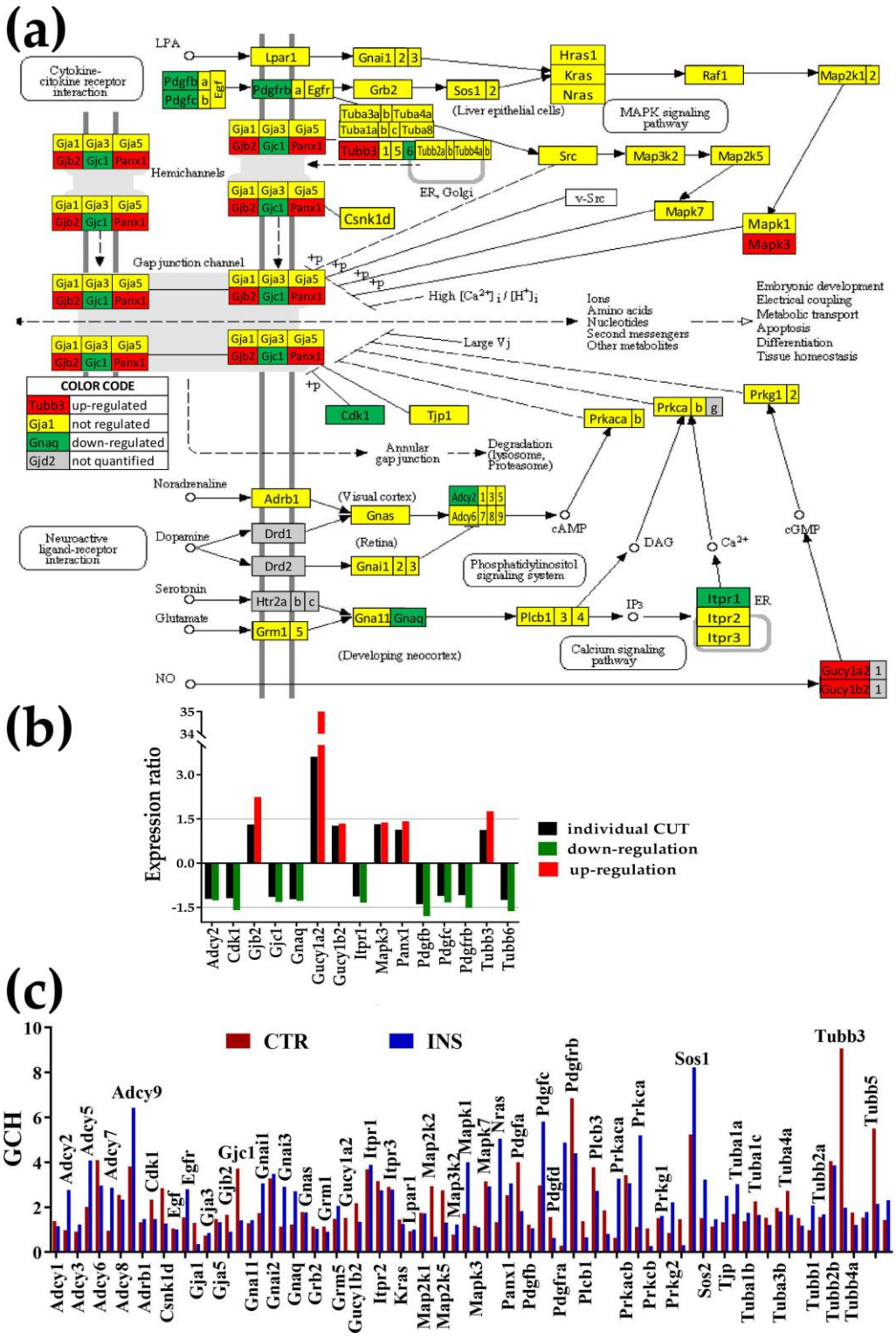

Figure 2. Presence of non-touching precursor oligodendrocytes affects genes in the gap junction (GJ) pathway (modified from https://www.genome.jp/kegg-bin/show_pathway?mmu04540).

(a) Regulation (up - red background, down – green background) of the interconnected genes within the GJ pathway. **(b)** Expression ratios and individual fold-change cut-offs (both negative for down-regulation) of the significantly regulated genes**. (c)** Gene Commanding Height (GCH) scores of the GJ genes in the two conditions. The most prominent gene in CTR astrocytes is *Tubb3* (GCH = 9.07), while in INS cells it is *Sos1* (GCH = 8.23). As illustrated in Fig. 1(c), considering the entire pathway, the median GCH increased by over 17% in INS with respect to CTR.

Significantly up-regulated genes in the GJ pathway were: gap junction protein, beta 2 (*Gjb2*, encoding Cx26), guanylate cyclase 1, soluble, alpha 2/beta 2 (*Gucy1a2/b2*), mitogen-activated protein kinase 3 (*Mapk3*), pannexin 1 (*Panx1*), tubulin, beta 3 class III (*Tubb3*).

Significantly down-regulated genes: adenylate cyclase 2 (*Adcy2*), cyclin-dependent kinase 1 (*Cdk1*), gap junction protein, gamma 1 (*Gjc1*, encoding Cx45), guanine nucleotide binding protein, alpha q polypeptide (*Gnaq*), inositol 1,4,5-trisphosphate receptor 1 (*Itpr1*), platelet derived growth factors (*Pdgfb, Pdgfc, Pdgfrb*), tubulin, beta 6 class V (*Tubb6*). Note that our method identified as significantly regulated *Adcy2*, *Gjc1*, *Gnaq*, *Gucy1b2*, *Itpr1*, *Mapk3*, *Panx1* and *Pdgfc* that would be neglected by the fixed uniform 1.5x cut-off. Even though the individual CUT for *Guc1a2* exceeded 1.5x due to high biological variability, the fold change was so large (!32-fold) that the difference was significant.

3.2.2. Significantly regulated cell-cycle genes

In Fig. 3, *Anapc2* (anaphase promoting complex subunit 2), *Mad2l2* (mitotic arrest deficient-like 2) and *Tgfb1* (transforming growth factor, beta 1) were the only significantly upregulated genes (however for both the fold-change was less than 1.5x).

Significantly down-regulated genes include: cell division cycles (*Cdc20, Cdc25A, Cdc6*), cyclins (*Ccna2, Ccnb2, Ccnd1*), cyclin-dependent kinases (*Cdk2, Cdk6*), cyclin-dependent kinase inhibitor 2A (*Cdkn2a*), DBF4 homolog (*Dbf4*), E2F transcription factors (*E2f1, E2f2*), growth arrest and DNA-damage-inducible 45 (*Gadd45a, Gadd45b*), minichromosome maintenance deficient (*Mcm2, Mcm4, Mcm6, Mcm7*), transformed mouse 3T3 cell double minute 2 (*Mdm2*), origin recognition complex subunits (*Orc2, Orc6*), protein kinase, membrane associated tyrosine/threonine 1 (*Pkmyt1*), polo-like kinase 1 (*Plk1*), RAD21 homolog (*Rad21*), retinoblastoma-like 1 (*Rbl1*), SMAD family member 2 (*Smad2*), structural maintenance of chromosomes 1A (Smc1a), transforming growth factor, beta 3 (*Tgfb3*), Ttk protein kinase (*Ttk*), WEE 1 homolog 1 (*Wee1*) and tyrosine 3-monooxygenase/tryptophan 5-monooxygenase activation protein, eta polypeptide (*Ywhah*).

3.2.3. Significantly regulated actin cytoskeleton genes

In the actin cytoskeleton pathway (Figure S1 in the Appendix) the up-regulated genes were chemokine (C-X-C motif) ligand 12 (*Cxcl12*), fibroblast growth factors (*Fgf1, Fgf9*), gelsolin (*Gsn*), integrins (*Itga9, Itgb2, Itgb4*), LIM-domain containing, protein kinase (*Limk1*), phosphatidylinositol-5-phosphate 4-kinase, type II, gamma (*Pip4k2c*), RAS-related C3 botulinum substrate 3 (*Rac3*), slingshot homolog 3 (*Ssh3*), WAS protein family, member 1 (*Wasf1*).

Down-regulated genes were actinin alpha 4 (*Actn4*), Rac/Cdc42 guanine nucleotide exchange factor 6 (*Arhgef6*), breast cancer anti-estrogen resistance 1 (*Bcar1*), Braf transforming gene (*Braf*), coagulation factor II (thrombin) receptor (*F2r*), guanine nucleotide binding protein (G protein), gamma 12 (*Gng12*), insulin II (*Ins2*), IQ motif containing GTPase activating proteins (*Iqgap1, Iqgap2, Iqgap3*), integrins (*Itga3 Itgav Itgb1, Itgb5*), lysophosphatidic acid receptor 4 (*Lpar4*), moesin (*Msn*), myosins (*Myh10, Myl12a, Myl2, Myl9*), p21 protein (Cdc42/Rac)-activated kinase 3 (*Pak3*), platelet derived growth factors (*Pdgfb, Pdgfc, Pdgfrb*). phosphatidylinositol 3-kinases (*Pik3ca, Pik3cb, Pik4k2a*), RAS viral (r-ras) oncogene homolog 2 (*Rras2*), vav 3 oncogene (*Vav3*), vinculin (*Vcl*).

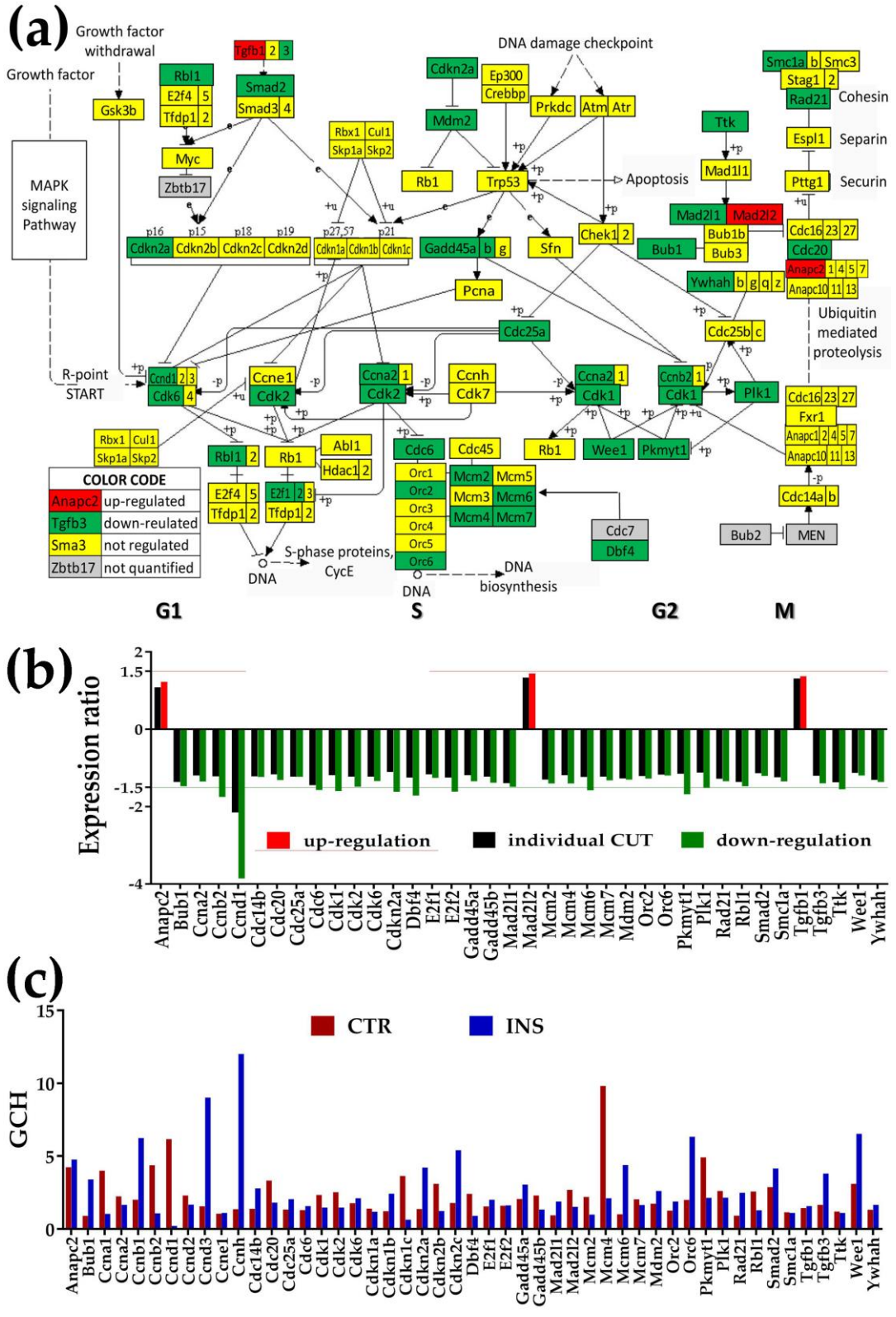

Figure 3. Presence of non-touching precursor oligodendrocytes affects cell-cycle (CC) pathway genes (modified from https://www.genome.jp/kegg-bin/show_pathway?mmu04110). **(a)** Regulation of the interconnected genes within the CC pathway. **(b)** Expression ratios and individual fold-change cut-offs (negative for down-regulation) of the significantly regulated genes. Note that the individual gene cut-off for *Ccnd1* (CUT = 2.152) exceeded 1.5x. **(c)** Gene Commanding Height (GCH) scores of the significantly regulated CC genes and other quantified cyclins (*Ccna1, Ccnb1, Ccnd2, Ccnd3, Ccne1, Ccnh*) and kinase inhibitors (*Cdkn1a, Cdkn1b, Cdkn1c, Cdkn2b, Cdkn2c*). *Mcm4* (GCH = 9.81) was the higest ranked CC gene in CTR and *Ccnh* (GCH = 12.01) the highest ranked CC

gene in cocultured astrocytes.

3.2.4. Significantly regulated genes responsible for the circadian rhythm

In the circadian rhythm pathway (Figure S2 in the Appendix) we found as significantly up-regulated only F-box and leucine-rich repeat protein 13 (*Fbxl13*) and as down-regulated: cryptochrome 1 photolyase-like (*Cry1*), period circadian clock 2 (*Per2*), protein kinase, AMP-activated, alpha 2 catalytic subunit (*Prkaa2*).

3.3. Regulation of signaling pathways

Figures 4-6 present the regulation of Ca^{2+}-, NOD-like receptor and thyroid hormone signaling pathways. The graphs below each pathway show the expression ratios and the individual cut-offs for the pathway genes that can be considered as significantly regulated, and the GCH scores of the regulated and other important genes. Where appropriate, we have shown also the genes whose variance was so high that even though they exceeded the traditional 1.5x in gene expression ratio, the differences were not statistically significant ("false hits").

3.3.1. Significantly regulated Ca^{2+}-signaling genes

In Figuure 4, the significantly up-regulated genes were**:** adenosine A2 receptors (*Adora2a, Adora2b*), calmodulin-like 4 (*Calml4*), cholecystokinin B receptor (*Cckbr*), CD38 antigen (*Cd38*), endothelin receptors a/b (*Ednr/b*), erb-b2 receptor tyrosine kinase 4 (*Erbb4*), 5-hydroxytryptamine (serotonin) receptor 5B (*Htr5b*), purinergic receptor P2X, ligand-gated ion channel, 6 (*P2rx6*), phosphodiesterase 1B, Ca2+-calmodulin dependent (*Pde1b*), phosphorylase kinases (*Phka2, Phkg1*), sphingosine kinase 2 (*Sphk2*).

Down-regulated genes were: adenylate cyclase 2 (*Adcy2*), adrenergic receptor, beta 3 (*Adrb3*), arginine vasopressin receptor 1A (Avpr1a), calcium channel, voltage-dependent, P/Q type, alpha 1A subunit (*Cacna1a*), calcium/calmodulin-dependent protein kinase II, delta (*Camk2d*), coagulation factor II (thrombin) receptor (*F2r*), guanine nucleotide binding proteins (Gna14, Gnaq), 5-hydroxytryptamine (serotonin) receptor 7 (*Htr7*), inositol 1,4,5-trisphosphate receptor 1 (*Itpr1*), purinergic receptor P2Y, G-protein coupled receptors (*P2ry1, P2ry2*), platelet derived growth factor receptor, beta polypeptide (*Pdgfrb*), prostaglandin F receptor (*Ptgfr*).

3.3.2. Significantly regulated NOD-like receptor signaling genes

In Figure 5, the significantly up-regulated genes were: cathelicidin antimicrobial peptide (*Camp*), chemokine (C-C motif) ligand 5 (*Ccl5*), conserved helix-loop-helix ubiquitous kinase (*Chuk*), cathepsin B (*Ctsb*), cytochrome b-245, beta polypeptide (*Cybb*), inhibitor of kappaB kinase epsilon (*Ikbke*), Janus kinase 1 (*Jak1*), mitogen-activated protein kinases (*Mapk13, Mapk3*), NLR family, apoptosis inhibitory protein 2 (*Naip2*), nucleotide-binding oligomerization domain containing 1 (*Nod1*), pannexin 1 (*Panx1*), RanBP-type and C3HC4-type zinc finger containing 1 (*Rbck1*), TGF-beta activated kinase 1/MAP3K7 binding protein 1 (*Tab1*), toll-like receptor adaptor molecule 1 (*Ticam1*), thioredoxin interacting protein (*Txnip*).

Significantly down-regulated genes were: anthrax toxin receptor 2 (*Antxr2*), B cell leukemia/lymphoma 2 (*Bcl2*), BCL2-like 1 (*Bcl2l1*), caspase 1 (*Casp1*), chemokine (C-C motif) ligand 12 (*Ccl12*), Fas (TNFRSF6)-associated via death domain (*Fadd*), guanylate binding protein 5 (*Gbp5*), inositol 1,4,5-trisphosphate receptor 1 (*Itpr1*), mitogen-activated protein kinases (*Mapk12, Mapk8*), receptor-interacting serine-threonine kinase 3 (*Ripk3*), signal transducer and activator of transcription 2 (*Stat2*), TANK-binding kinase 1 (*Tbk1*), transient receptor potential cation channel, subfamily V, member 2 (*Trpv2*).

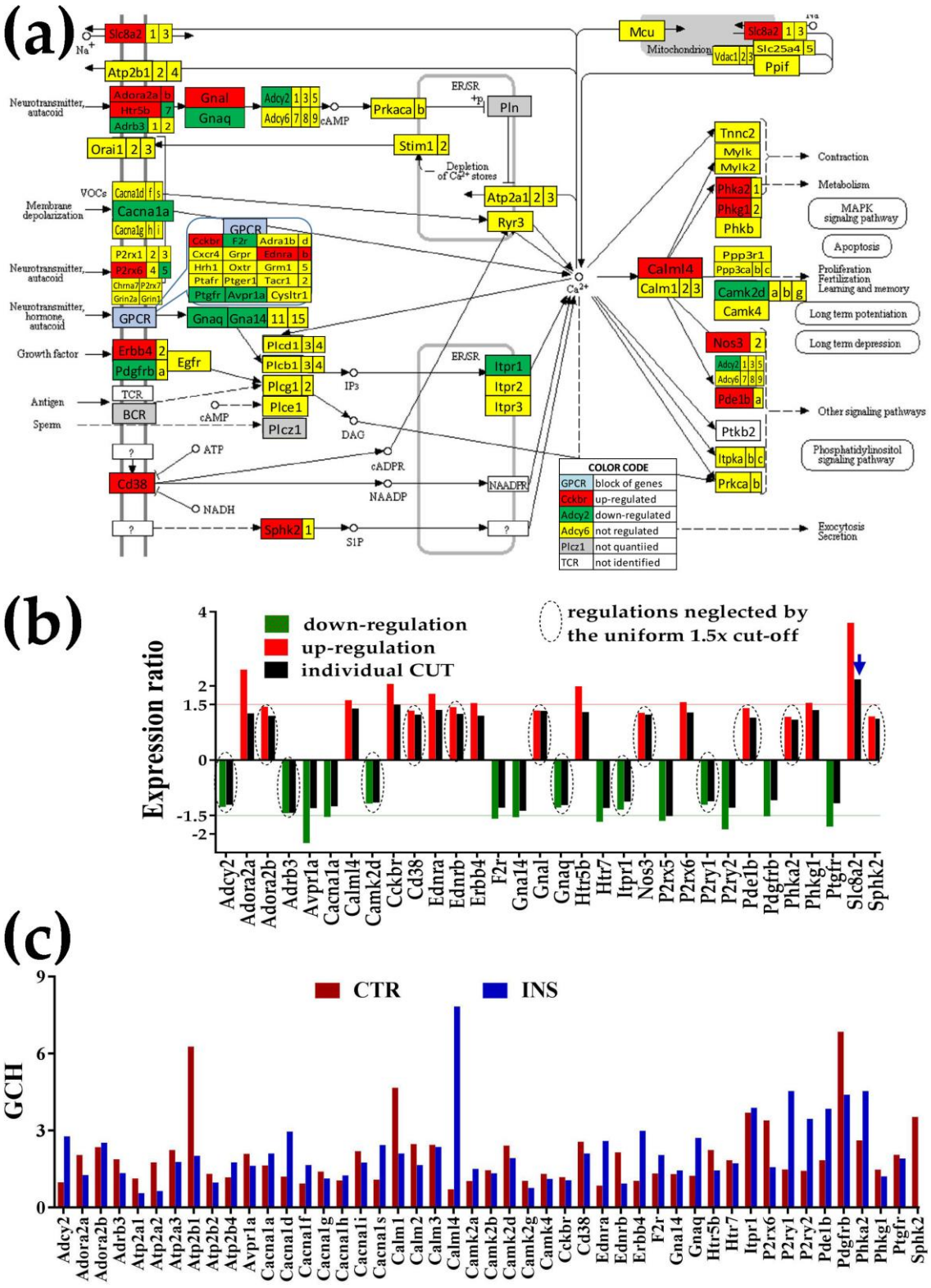

Figure 4: Presence of non-touching precursor oligodendrocytes regulates calcium-signaling (CAS) pathway in astrocytes (modified from mmu04020, www.kegg.jp). **(a)** Regulation of interconnected genes within the CAS pathway. **(b)** Expression ratios and individual fold-change cut-offs (negative for down-regulation) of the significantly regulated genes. Note that 14 out of 32 significantly regulated genes had absolute fold-changes below the traditional 1.5x and that CUT exceeded 1.5x for *Slc8a2*. **(c)** Gene Commanding Height (GCH) scores of selected CAS genes. Owing to their recognized importance, in **4(c)** the set of the significantly regulated CAS genes was completed with:

Ca^{2+}-transporting ATPases (*Atp2a1*, *Atp2a2*, *Atp2a3*, *Atp2b1*, *Atp2b2*, *Atp2b4*), calcium channels (*Cacna1d*, *Cacna1f*, *Cacna1g*, *Cacna1h*, *Cacna1i*, *Cacna1s*), calmodulins (*Calm1*, *Calm2*, *Calm3*) and calcium/calmodulin-dependent protein kinases (*Camk2a*, *Camk2b*, *Camk2g*, *Camk4*).

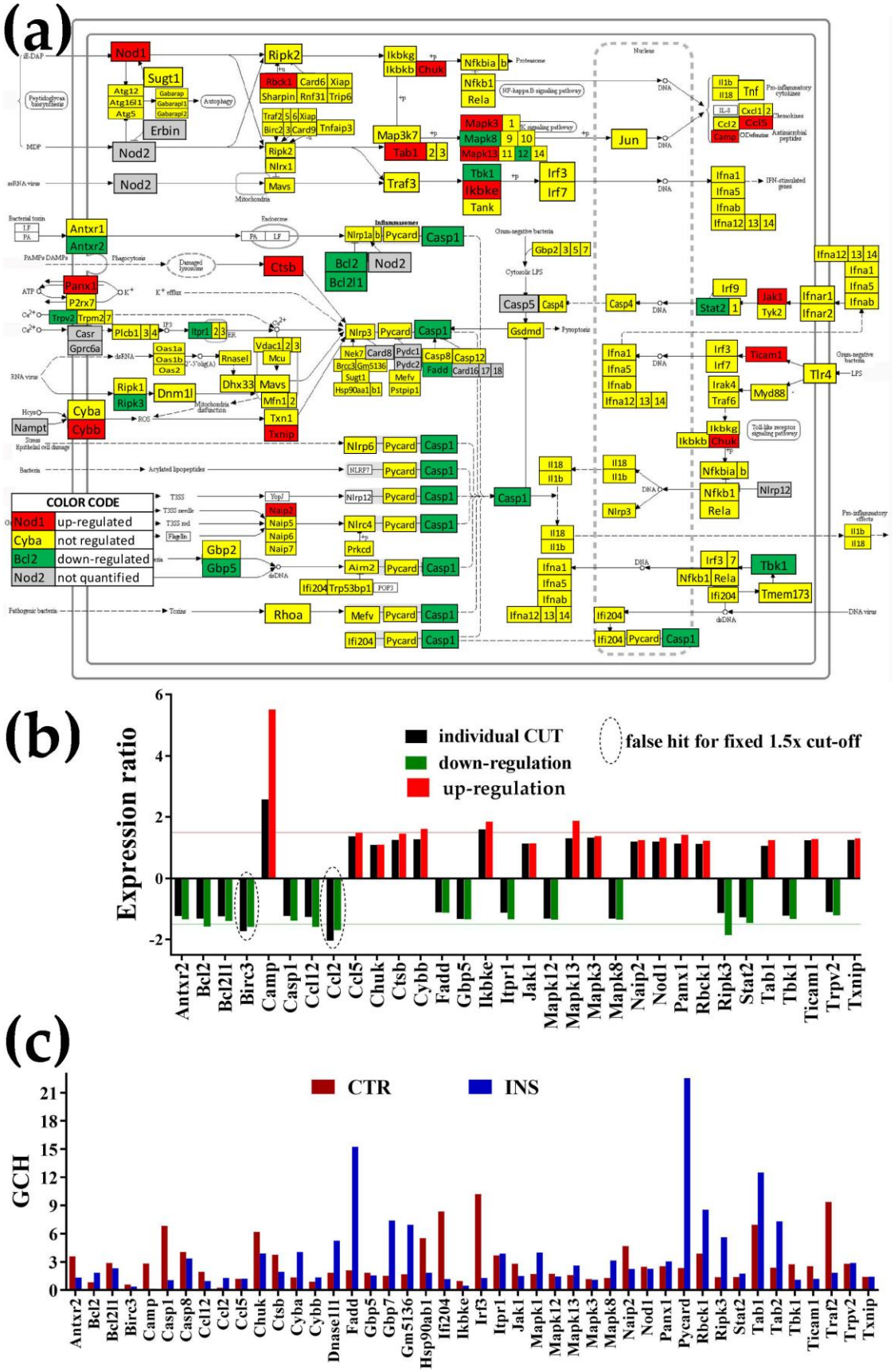

Figure 5: Proximity of non-touching precursor oligodendrocytes affects the NOD-like receptor signaling pathway (modified from http://www.kegg.jp/pathway/mmu04621). **(a)** Regulation of interconnected genes. **(b)** Expression ratios and individual fold-change cut-offs (negative for down-regulation) of the significantly regulated genes. Note that *Birc3* and *Ccl12* would be false hits if the traditional 1.5x were used instead of our individual gene cut-off because although their expression ratios were over the 1.5x limit, they did not exceed their individual CUT. **(c)** Gene Commanding Height (GCH) scores of selected NOD genes. The set of the significantly regulated NOD genes was completed with genes having GCH over 4 in either condition: *Casp8, Cyba, Dnase1l1, Gbp7, Gm5136,* heat shock protein (*Hsp90aa1*), interferon regulatory factor (*Irf3*), mitogen-activated protein kinase (*Mapk1*), PYD and CARD domain containing (*Pycard*, the most prominent of the NOD pathway in the INS astrocytes), *Tab2, Traf2*.

3.3.3. Significantly regulated thyroid hormone signaling genes

In Figure 6, the significantly up-regulated genes were: ATPase, Na+/K+ transporters (*Atp1a2, Atp1b2*), deiodinase, iodothyronine, type II (Dio2), forkhead box O1 (*Foxo1*), Mapk3, mediator complex subunits (*Med13l, Med24*), myosin, heavy polypeptide 6, cardiac muscle, alpha (*Myh6*), solute carrier family 2 (facilitated glucose transporter), member 1 (*Slc2a1*), tuberous sclerosis 2 (*Tsc2*).

Significantly down-regulated genes were: ATPase, Na+/K+ transporting, alpha 4 polypeptide (*Atp1a4*), bone morphogenetic protein 4 (*Bmp4*), cyclin D1 (*Ccnd1*), catenin (cadherin associated protein) beta 1 (*Ctnnb1*), hypoxia inducible factor 1 alpha subunit (*Hif1a*), integrin alpha V (*Itgav*), transformed mouse 3T3 cell double minute 2 (*Mdm2*), mediator complex subunit 30 (*Med30*), phosphatidylinositol 3-kinases (*Pik3ca, Pik3cb*), regulators of calcineurin (*Rcan1, Rcan2*), solute carrier family 16 (monocarboxylic acid transporters) member 10 (*Slc16a10*), thyroid hormone receptor beta (*Thrb*).

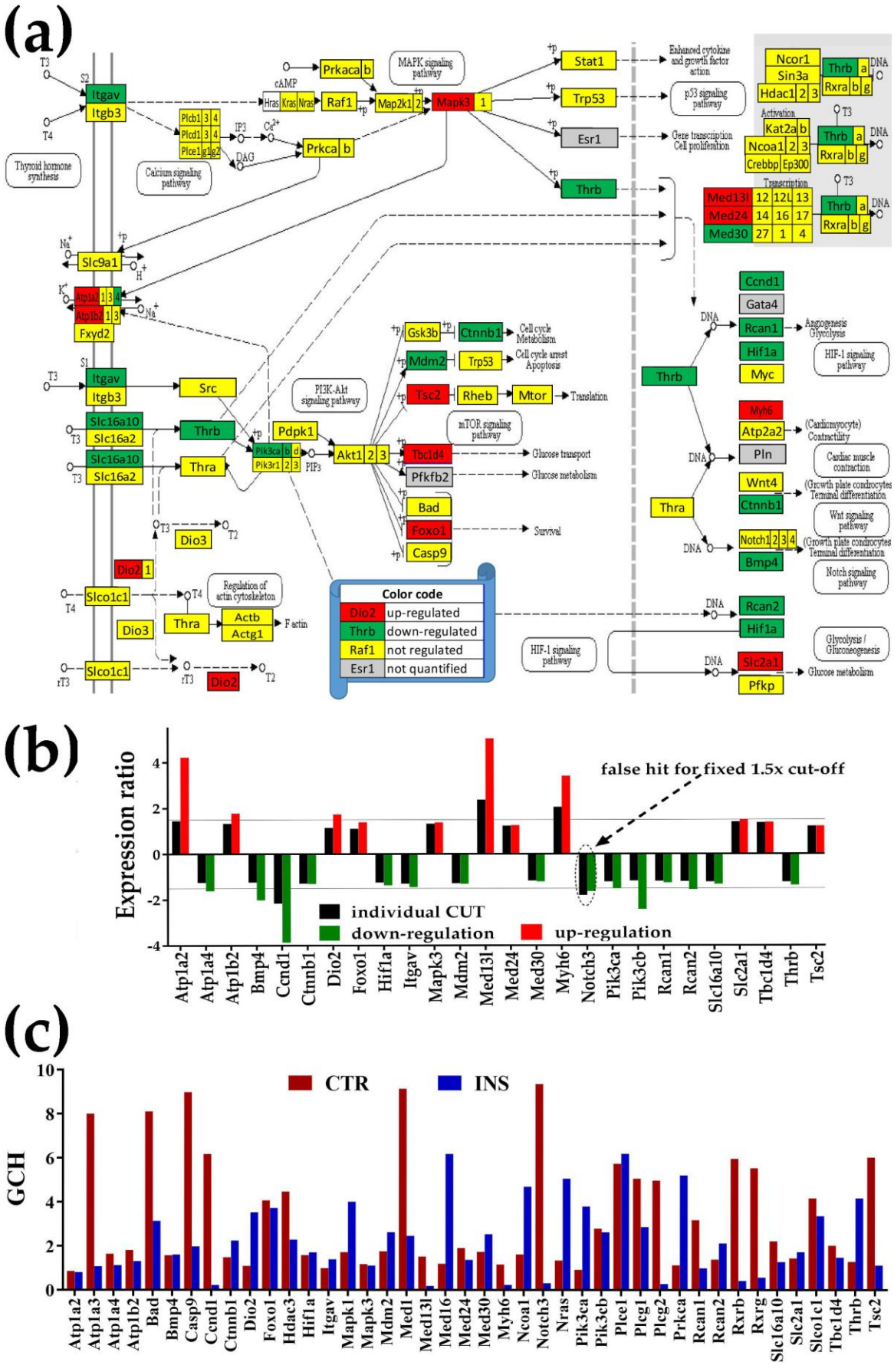

Figure 6: Proximity of non-touching precursor oligodendrocytes affects the thyroid hormone signaling pathway (modified from http://www.kegg.jp/pathway/mmu04919). **(a)** Significantly

regulated genes. **(b)** Expression ratios and individual fold-change cut-offs (negative for down-regulation) of the significantly regulated genes. Note that *Notch3* would be a false hit if the traditional 1.5x would be used instead of our individual gene cut-off because although the absolute expression ratio exceeded 1.5x it was below the individual gene CUT. **(c)** Gene Commanding Height (GCH) scores of selected TH genes. In addition to the significantly regulated TH genes, we plotted genes with high GCH scores in one condition: Na^+/K^+ transporting , alpha 3 polypeptide (*Atp1a3*), BCL2-associated agonist of cell death (*Bad*), caspase 9 (Casp9), subunits of mediator complex (*Med1, Med16*), notch 3 (*Notch3*), parathyroid hormone 1 receptor (*Pth1r*), regulators of calcineurin (*Rcan1, Rcan2*), and thyroid hormone receptor associated protein 3 (*Thrap3*).

3.4. Oligodendrocyte proximity remodels the integration of astrocytes with neighboring, synaptically coupled neurons

As illustrated in Figure 7, oligodendrocytes have an indirect modulatory role on the astrocyte response to the release of neurotransmitters in the synaptic cleft. Interestingly, the astrocytes cultured in the presence of non-touching oligodentryocytes exhibited primarily up-regulated genes related to the glutamatergic (*Glul, Grm3)*, GABAergic (*Glul)* and dopaminergic (*Maob)* transmission, whereas their expression of serotonin markers tended to be lower (*Itpr1l, Gnaq, Trpc1).* We found no significant change in the control of the cholinergic synapse.

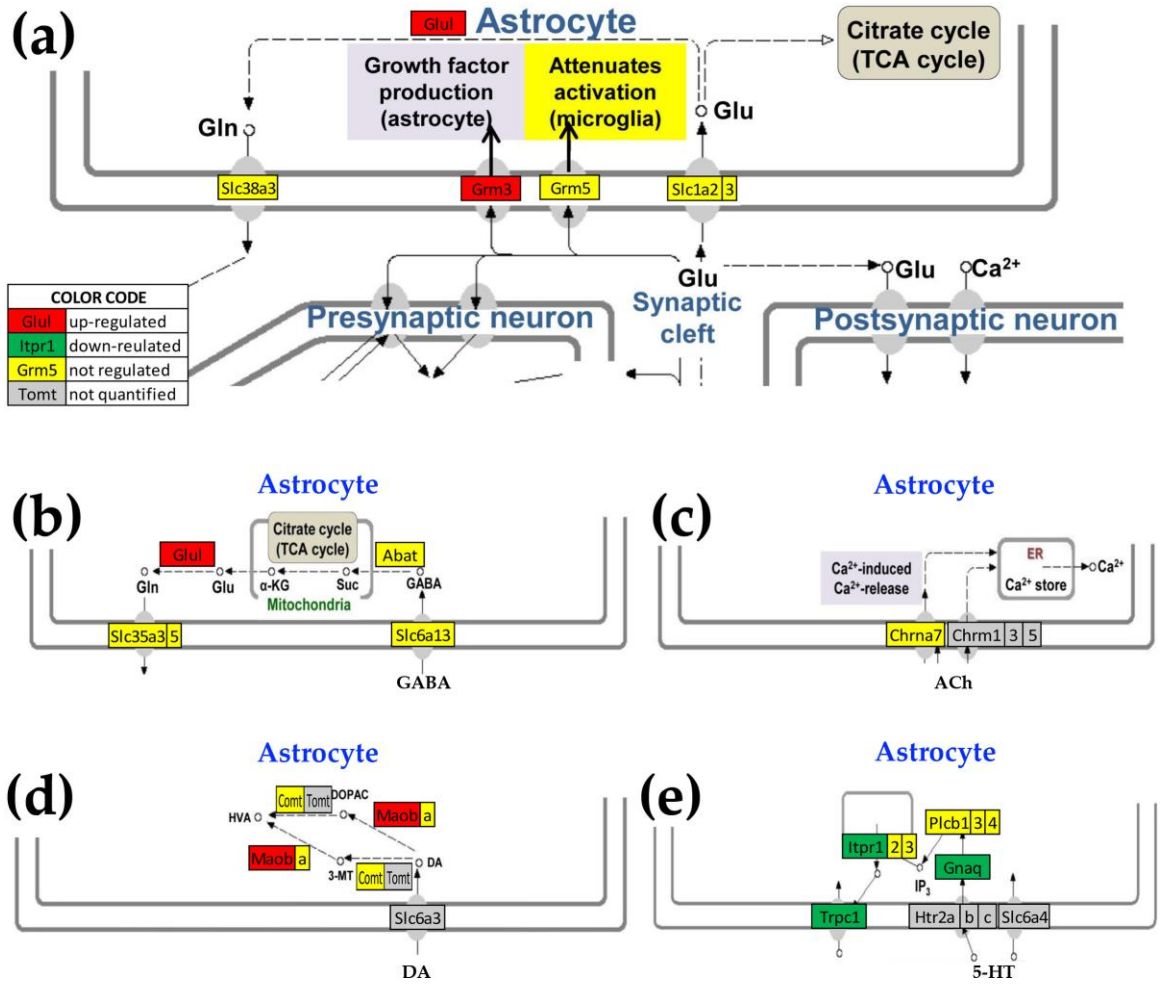

Figure 7: Astrocyte genes that respond to synaptic neurotransmission were altered by oligodendrocyte presence. Panels present the genes whose encoded proteins in the astrocyte membrane are interacting with the proteins from the pre- and post-synaptic neurons. **(a)** glutamatergic synapse (modified from mmu04724, kegg.jp), **(b)** GABAergic synapse (modified from mmu04727, kegg.jp), **(c)** cholinergic synapse (modified from mmu04725, kegg.jp), **(d)** dopaminergic synapse (modified from mmu04728, kegg.jp), **(e)** serotonergic synapse (modified from mmu04726, kegg.jp). Genes: 4-aminobutyrate aminotransferase (*Abat*), cholinergic receptor, nicotinic, alpha polypeptide 7 (*Chrna7*), catechol-O-methyltransferase (*Comt*), glutamate-ammonia ligase (*Glul*), guanine nucleotide binding protein, alpha q polypeptide (*Gnaq*), metabotropic glutamate receptors (*Grm3*, *Grm5*), inositol 1,4,5-trisphosphate receptors (*Itpr1, Itpr2, Itpr3*), monoamine oxidases (*Maoa, Maob*), beta phospholipases C (*Plcb1, Plcb2, Plcb3*), solute carriers (*Slc1a2, Slc1a3, Slc35a3, Slc35a5, Slc38a3, Slc6a13*), and transient receptor potential cation channel, subfamily C, member 1 (*Trpc1*).

3.5. Cellular environment remodels gene networks

We found that, in addition to regulating numerous individual genes, oligodendrocytes proximity had a major impact on the gene networks. Figure 8 illustrates this finding by the changes in the coordinated expression of *Gja1* and *Panx1* (encoding the intercellular major gap junction channel forming protein Cx43), and the ATP release channel protein Panx1) with actin-cytoskeleton (8a) and circadian rhythm (8b) genes. Both Cx43 and Panx1 are well-documented for their important roles in the physio-pathology of the Central Nervous System [52,53]. This analysis shows that the expression synergism of *Panx1* with *Fgf18, Itga2b* and *Pdgfd* in isolated (control) astrocytes was reversed to an antagonistic coordination by the proximity of *Oli-neu* cells (in insert), while the antagonism of *Gja1* with *Pip4k2b* was turned into synergism. Interestingly, expression level of *Gja1* was practically not affected by the presence of oligodendrocytes (the 7% observed reduction is below the corresponding cut-off) but that of *Panx1* was increased by more than 42%. More interesting is that the synergistic expression of *Gja1* with the actin-cytoskeleton genes increased by 30%, the independent expression stayed the same (3.4%) and the antagonistic expression decreased by 11%. However, the proximity of oligodendrocytes turned the very different coordination patterns of *Gja1* and *Panx1* with circadian rhythm genes in CTR astrocytes into practically identical ones (i.e. the two genes encoding channel forming proteins are similarly related to the circadian rhythm genes).

Interestingly, the negative coordination of *Gja1* with *Pip4k2b* (phosphatidylinositol-5-phosphate 4-kinase, type II, beta) in CTR astrocytes was switched to a positive one in INS astrocytes. By contrast, the expression synergisms of *Panx1* with *Fgf18* (fibroblast growth factor 18), *Itga2b* (integrin alpha 2b) and *Pdgfd* (platelet derived growth factor, B polypeptide) in CTR were reversed into antagonistic ones in INS.

The findings that co-culture of astrocytes with *Oli-neu* cells results in transcriptomic remodeling of a number of functional pathways led us to examine whether the presence of astrocytes in co-culture with the oligodendrocyte precursor cells would also result in remodeling of the oligodendrocyte gene networks. To test this hypothesis, we reanalyzed the expression data from a previous experiment profiling the oligodendrocytes cultured alone or co-cultured with astrocytes in the same experimental set up [29,30]. Figures 8(c) and 8(d) illustrate the remodeling of the expression coordination of *Panx1* with the same actin cytoskeleton and circadian rhythm genes

in the oligodendrocytes cultured alone (Oli – Ast) or with non-touching astrocytes in the neighborhood (Oli + Ast). *Gja1* coordination partners are shown for astrocytes but not for oligodendrocytes which do not express Cx43.

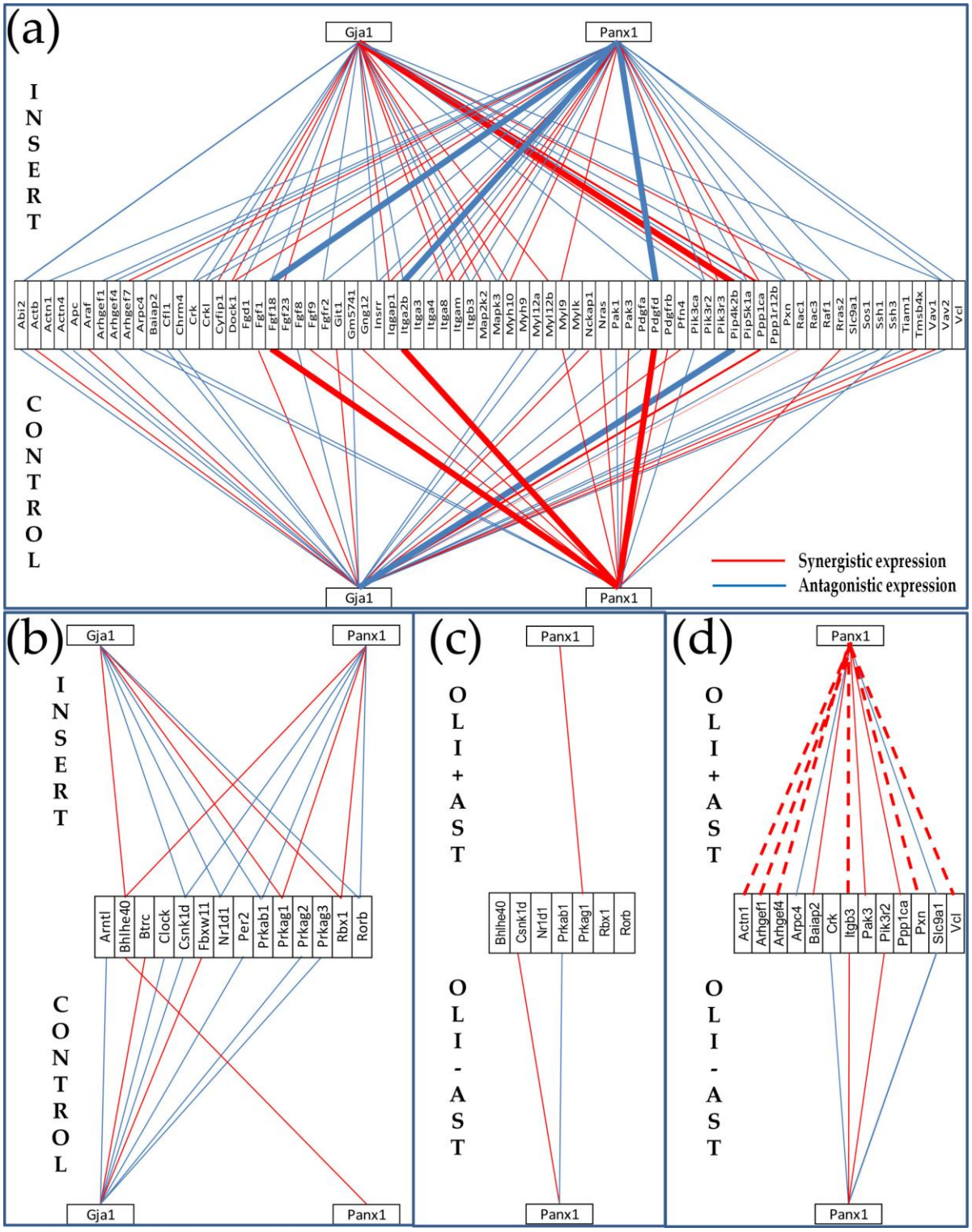

Figure 8: Topology of gene networks is sensitive to the cellular environment. **(a-b)** Proximity of non-touching precursor oligodendrocytes remodels the transcriptomic networks by which expression of genes encoding connexin43 (*Gja1*) and pannexin1 (*Panx1*) relate to the expression of **(a)** actin cytoskeleton and **(b)** circadian rhythm genes in astrocytes. **(c-d)** Proximity of non-touching

astrocytes changes the expression coordination of *Panx1* with **(c)** circadian rhythm and **(d)** actin cytoskeleton genes in oligodendrocytes. Thicker continuous lines in **8(a)** indicate reversal type of coordination in astrocyte by oligodendrocyte proximity. Dashed lines in **8(d)**indicate opposite coordination in astrocytes and oligodendrocytes when co-cultured. **CONTROL/OLI-AST** = astrocytes/oligodendrocytes cultured alone. **INSERT/OLI+AST** = co-culture of astrocytes and oligodendrocytes. Note: in order to simplify the illustration, only the *Panx1* coordination partners from the two pathways in astrocytes were presented in oligodendrocytes.

Among the most striking differences in the co-cultured cells were that the negative coordination of *Panx1* with *Actn1* (actinin alpha 1), *Arghef1/4* (Rho guanine nucleotide exchange factor (GEF) 1/4), *Itgb3* (integrin beta 3), *Pxn* (paxillin) and *Vcl* (vinculin) in astrocytes were positive in oligodendrocytes. This finding indicates that, at least for the actin cytoskeleton, *Panx1* plays opposite roles in the two types of glial cells.

4. **Discussion**

In two previously published papers, we have shown that astrocyte-conditioned medium is a major regulator of gene expression in oligodendrocytes even in the absence of cytosol-to-cytosol communication via gap junction channels connecting these two cell types [29,30]. In the present study, we analyzed whether oligodendrocyte-conditioned medium changes significantly the astrocyte transcriptome. Together with our studies on brains of Cx43KO, Cx32KO and Cx36 mice [7-11], these data on astrocytes and oligodendrocytes cultured alone and co-cultured with each-other show the transcriptomic integration of the brain glia.

Our experimental results show that glial integration persists even in the absence of direct astrocyte-oligodendrocyte communication via gap junction channels The regulation of genes that modulate the neurotransmission suggests that neurons may be also part of the transcriptomic integration. Until now, no gap junction channel was found between neurons and astrocytes or oligodendrocytes in the mouse brain. However, formation of functional neuron-glia gap junction channels has so far been identified between somata of peripheral sensory ganglia neurons and surrounding satellite glial cells [54]. There are also reports of glia-neuronal gap junctions in *C. elegans* [55]. Nevertheless, integration of neurons with glial cells can be carried out by molecules released by one cell type binding membrane receptors of other cell type as reported by many authors (e.g. [56-8]). It can be also acquired via transfer of exosomes [59].

Microarray data were analyzed from several, complementary perspectives, considering all three independent expression features that can be determined from studies incorporating four biological replicas. The study was empowered by advanced analytical approaches. For instance, as listed in Supplementary Table S1, our method eliminated the “false hits” (absolute fold-change over 1.5x but below CUT). However, we have determined that some of the “false negatives” were actually significantly regulated (absolute fold-change less than 1.5x but over CUT), listed in Supplementary Tables S2 and S3. Moreover, the traditional percentage of significantly regulated genes was complemented with the Weighted Pathway Regulation (WPR). WPR weighs the contribution of each regulated gene with respect to a cut-off tailored for it by considering the technical noise and biological variability. Of note in Fig. 1a is that, from the perspective of the WPR score, the gap junction (GJ) pathway was more affected than the others (WPR = 43.3), indicating that

Oli-neu proximity exerted major impact on hetero-cellular communication even in the absence of cell-to-cell contact.

In the case of CC, the much larger percentage of down-regulated genes suggests a slow-down of the mitotic progression of astrocytes in the vicinity of oligodendrocytes that we have observed but have not yet quantified.

Relative Expression Variability (REV) shows the vulnerability of the gene expression in response to even subtle (not regulating) environmental changes. Very low REV (expression level fluctuates within very narrow interval across biological replicates) indicates strong control of transcript abundance exerted by homeostatic mechanisms, most likely reflecting survival advantage afforded by proportional expression levels of the genes. Whereas strictly controlled genes likely reflect those that are critical for cell survival or phenotypic expression, genes with high REV may represent ones that are more susceptible to adaptation to environmental fluctuations.

In several other transcriptomic studies we found an overall reduction of gene REV in cells and tissues collected from subjects with various diseases (epilepsy [60], experimental autoimmune encephalomyelitis [61], kidney cancer [62]) compared to healthy counterparts. REV was also significantly lower in tissues from animals subjected to various stresses (microgravity [63], chronic hypoxia [64-6]) or genetic manipulations (e.g. [7,33]. The consistency of these findings suggest that the overall higher expression variability seen in astrocytes co-cultured with *Oli-neu* cells indicates that the proximity of oligodendrocytes provide an environment that is closer to that of their physiological state than when astrocytes are cultured alone.

GCH indicates the degree to which expression of a gene influences the expression stability and interconnectivity of the functional pathway in that condition. While the GCH analysis confirmed the known impact of some genes, for others additional experiments may be needed to understand their role in the pathway. Since GCH was derived from measures of expression control and coordination that are independent between each-other and from the average expression levels, correspondence between genes with high GCH in anyone condition and their significant regulation in the other is just casual. However, experimental alteration of a gene is expected to have transcriptomic consequences in line with its GCH. We confirmed this hypothesis by stably lentiviral transfecting each of two different human thyroid cancer cell lines (papillary BCPAP and anaplastic 850C) with the same gene (*DDX19B, NEMP1, PANK2, UBALD1*) [50,51]. Interestingly, the top gene (highest GCH) in one condition scores very low in the other. Thus, *Serp2* has GCH = 49.31 in CTR astrocytes but GCH = 2.49 in INS astrocytes, while *Pdcd7* has GCH = 48.13 and GCH = 2.14 in CTR astrocytes. The high level of *Serp2* suggests that it plays a critical role for the regulation of transcription and translation to protect against ER stress caused by the accumulation of unfolded proteins [67,68]. The much higher ranking of *Pdcd7* (GCH = 48.13 in INS astrocytes compared to GCH = 2.14 in CTR astrocytes), highlights the importance of controlling the astrocyte proliferation [69] during brain development and formation of the normal cellular environment (that contains also precursor oligodendrocytes).

The prominence of *Tubb3* in the GJ pathway of CTR astrocytes confirms its role in cytoskeletal adaptation of microtubules in astrocytes cultured without any other cells [70], while that of *Sos*1 in astrocytes co-cultured with oligodendrocytes shows its prevalence with regard to cell proliferation and viability [71]. Interestingly, all three cell-cycle genes from the *Ccnh.Cdk7.Pea15a* complex [72] of the basal transcription factor TFIIH are almost equally low positioned in cultured alone astrocytes (GCH_{CTR} = 1.36 (*Ccnh*), 1.63 (*Cdk7*), 1.88 (*Pea15a*)). However, in the presence of oligodendrocytes *Ccnh*

is promoted to the top position in this pathway (GCH_{INS} = 12.01), while the other two genes of the complex stayed closed to their initial place: 1.45 (*Cdk7*), 1.65 (*Pea15a*)). The high position of *Ccnh* in an environment closer to that of the brain can explain why the Ex8+49T>C variant of this gene is associated with increased risk of glioma [73].

We found that several members of the gap junction pathway related genes (including *Gjb2*, encoding Cx26) were differentially expressed in astrocytes in the presence of *Oli-neu* cells (Figure 2). However, to our surprise, the expression of the main connexin gene, *Gja1*, was not affected, although the astrocytes should have sensed the presence of the oligodendrocytes in the neighborhood. This result is surprising because the oligodendrocytes responded to the presence of astrocytes by increasing the expression of *Gjc2* (encoding Cx47), the Cx43 partner in heterocellular gap junction channels [74], by 9.70x. We determined the up-regulation of *Gjc2* by re-analyzing the previously reported microarray data on *Oli-neu* with the same set up [29,30]. It should be noted that increased expression levels for gap junction proteins are not always matched with changes in coupling. There is variation in astrocyte-astrocyte coupling as well as astrocyte-oligodendrocyte coupling. Intra-astrocyte gap junctions (a.k.a reflexive or autaptic gap junctions) seems to be common but has barely been studied. Given the preceding considerations and that Cx43 expression in astrocytes is very high in comparison to most other brain proteins, we predict that the non-significantly changed Cx43 expression is compatible with increased oligodendrocyte Cx47 (and presumably resulting in higher astrocyte-oligodendrocyte coupling). Nevertheless, the overexpression of *Gjb2* in astrocytes can also be related to the up-regulation of *Gjc2* in oligodendrocytes, confirming the potential coupling of the encoded connexins [75].

Interestingly, by regulating the astrocyte transcriptome, as illustrated in Fig.7, the proximity of oligodendrocytes modulates also the bidirectional interactions of astrocytes with the inter-neuronal synapses [76] that are essential for the development of cortical circuits [77].

The coordination patterns of *Panx1* illustrate the degree to which gene networks can be remodeled in response to environmental factors. *Panx1* has mostly synergistic coordination with actin cytoskeleton genes in astrocytes cultured alone, whereas it is antagonistically coordinated with these genes when cocultured with oligodendrocytes (Fig.8a). Conversely, oligodendrocyte actin genes are largely independent of *Panx1* when cultured alone but become synergistically coordinated with *Panx1* when cultured with astrocytes (Fig.8d). The opposite consequences of coculture on *Panx1*-coordinated cytoskeleton related genes in astrocytes and oligodendrocytes might reflect fundamental divergence in maturation or/and response to inflammatory stimuli.

A distinct type of network remodeling is exemplified by the mostly antagonistic coordinations of *Gja1* with circadian rhythm genes in cultured alone astrocytes, with almost no coordination for *Panx1*. In coculture, antagonistic and synergistic coordinations with Gja1 are approximately equal, while each coordination is matched by a similar coordination with *Panx1*. Thus, these two maxi channel proteins act independently on circadian rhythm genes of astrocytes alone but become cooperative and may compensate for one another when in the presence of oligodendrocytes. Interestingly, we reported that the coordination patterns of *Gja1* and *Panx1* with the whole brain transcriptome of wild type mice were highly (90.8%) similar [9].

Therefore, because of their involvement in sleep pressure and the demonstrated ability for astrocytes to control neuron activity in the suprachiasmatic nucleus of the hypothalamus along with the hippocampus [78-80], we tested for an effect of oligodendrocytes on transcription of genes

linked to circadian rhythm. The general trend is down-regulation of genes that control circadian cycling of downstream transcriptional regulators with upregulation of the circadian cycle dampening gene *Fbxl13* (F-box and leucine-rich repeat protein 13). *Fbxl13* has been implicated in increasing ubiquitination and degradation of cryptochrome proteins, including *Cry1*, through ubiquitin-protein ligase activity of Fbxl13 with over-expression of *Fbxl13* producing enhanced degradation of Cry1 and Cry2 [81]. We found that the presence of nearby oligodendrocytes significantly up-regulated *Fbxl13* by 2.59x, down-regulated *Cry1* by -1.23x (CUT = 1.19x) and left unchanged *Cry2*. The effects on the circadian rhythm pathway point to more rapid or dampened cycling. Strikingly, knockout of Cx43 (along with Cx30) in astrocytes disrupted circadian rhythm and produced higher circadian rhythm amplitude [82]. The finding of increased expression of *Gjb2* and *Fbxl13* in astrocytes grown in the presence of *Oli-neu* cells might be a starting point for understanding the role of astrocyte connexins in controlling circadian rhythm.

A recent study [83] indicated that astrocytes can drive circadian related gene cycling in neurons of the suprachiasmiatic nucleus. Astrocyte gap junctions have been shown to affect and be affected by wakefulness [84]. Our results show that co-culturing substantially increased the coordination of *Panx1* with circadian rhythm genes in the astrocytes but has practically no consequences for the oligodendrocytes.

The perivascular end-feet of astrocytes have been implicated in the uptake of thyroid hormones, especially thyroxine (T4) which is the vastly predominant, but mostly inactive form of thyroid hormone in the blood. After T4 is transported through brain endothelial cells it is thought to be mainly brought into astrocytes by transporters with varying specificity for T4. Once taken into astrocytes, T4 is converted to the highly active form triiodothyronine (T3) by iodothyronine deiodinase type 2 (DIO2) with *DIO2* mRNA expression largely exclusive to astrocytes as reviewed in [85]. Taken together, the preceding aspects of thyroid handling point to astrocytes as key uptake and distribution cells in the brain. Additionally, oligodendrocyte maturation and key myelin production gene expression is strongly regulated (promoted) by T3 [86,87] Therefore, thyroid hormone handling pathway is important to oligodendrocytes and their precursors leading us to examine our data for changes astrocyte thyroid pathway genes in response to the presence of non-contacting *Oli-neu* cells. The presence of *Oli-neu* cells decreased expression of *Slc16a10* (*Mct10*) but did not produce a change in the other two transporters expressed in astrocytes: *Slo1c1* (OATP1C1) and *Slc16a2* (MCT8). More interestingly, *Dio2* was upregulated in the presence of Oli-neu cells. *Tbc1d4* is upregulated in astrocytes cultured in the presence of Oli-neu cells and this GTPase increases surface expression of glucose transporters [88]. These results may indicate a shift towards an astrocyte phenotype that may produce activated thyroid hormone and bring in additional glucose. It is interesting to speculate that the presence of Oli-neu cells produces gene expression changes in astrocytes that would support myelination through increased production of activated T3 and support of the high metabolic demands of myelinating oligodendrocytes.

5. Conclusions

The major caveat of this study is that the *oli-neu* cells are not the natural but the immortalized precursor oligodendrocytes. However, our results clearly indicate that the cellular environment plays an integrative role by modulating the expression level, the expression control and the

expression coordination of the genes in each and every cell phenotype of a heterogeneous tissue like brain. Because of this, one should be very cautious when extending the observations from homocellular cultures to the behavior of the same cell phenotypes within a heterocellular tissue.

Supplementary Materials: The following are available online at www.mdpi.com/xxx/s1. Table S1: Genes whose >1.5x absolute fold-change did not meet the individual CUT criterion. Red/green background of the expression ratio indicates not significant (false) up-/down-regulation. Table S2: Genes considered as significantly up-regulated although their absolute fold-change was below the traditional 1.5x. Table S3: Genes considered as significantly down-regulated although their absolute fold-change was below the traditional 1.5x. Figure S1: Presence of non-touching precursor oligodendrocytes regulate the actin cytoskeleton (AC) pathway. Figure S2: Presence of non-touching precursor oligodendrocytes regulates the Circadian Rhythm (CR) pathway,

Author Contributions: Conceptualization, D.A.I. and D.C.S.; methodology, D.A.I. and S.I.; software, D.A.I,; validation, D.A.I. and S.I.; formal analysis, D.A.I. and S.I.; investigation, S.I. and D.A.I.; resources, D.C.S. and D.A.I.; data curation, D.A.I.; writing—original draft preparation, D.A.I.; writing—review and editing, R.S. and D.C.S.; visualization, D.A.I..; supervision, D.A.I. and D.C.S.; project administration, D.A.I.; funding acquisition, D.A.I. All authors have read and agreed to the published version of the manuscript

Funding: D.A.I. was supported by the TAMUS Chancellor's Research Initiative (CRI) funding for the Center for Computational Systems Biology at the Prairie View A&M University, D.C.S. was supported by the NIH grants NS092466 and NS092786. R.S. was supported by NYIT-COM In-House Grant for gap junction research.

Acknowledgments: The Oli-neu cell line was kindly provided by Dr. J. Trotter (University of Mainz, Germany)

Conflicts of Interest: The authors declare no conflict of interest. The funders had no role in the design of the study; in the collection, analyses, or interpretation of data; in the writing of the manuscript, or in the decision to publish the results.

References

1. Fields, R.D. White matter in learning, cognition and psychiatric disorders. *Trends Neurosci* **2008**, 31, 361–370. DOI: 10.1016/j.tins.2008.04.001
2. Filley, C.M.; Fields, R.D. White matter and cognition: making the connection. *J Neurophysiol* **2016**, 116(5):2093-2104. DOI: 10.1152/jn.00221.2016
3. Stogsdill, J.A.; Eroglu, C. The interplay between neurons and glia in synapse development and plasticity. *Curr Opin Neurobiol* **2017**, 42(1-8). DOI: 10.1016/j.conb.2016.09.016
4. Fasciani, I.; , Pluta, P., González-Nieto, D.; Martínez-Montero P.; Molano, J.; Paíno, C.L. et al. Directional coupling of oligodendrocyte connexin-47 and astrocyte connexin-43 gap junctions. *Glia* **2018**, 66(11):2340-2352. DOI: 10.1002/glia.23471
5. Claus, L.; Philippot, C.; Griemsmann, S.; Timmermann, A.; Jabs, R.; Henneberger, C. et al. Barreloid Borders and Neuronal Activity Shape Panglial Gap Junction-Coupled Networks in the Mouse Thalamus. *Cereb Cortex* **2018**, 28(1):213-222. DOI: 10.1093/cercor/bhw368
6. Augustin, V.; Bold, C.; Wadle, S.L.; Langer, J.; Jabs, R.; Philippot, C. et al. Functional anisotropic panglial networks in the lateral superior olive. *Glia* **2016**, 64(11):1892-911. DOI: 10.1002/glia.23031.
7. Iacobas, D.A.; Scemes, E.; Spray, D.C. Gene expression alterations in connexin null mice extend beyond the gap junction. *Neurochem. Intl* **2004**,, 45(2-3), 243-250. DOI: 10.1016/j.neuint.2003.12.008.
8. Iacobas, D.A.; Iacobas, S.; Urban-Maldonado, M.; Spray, D.C. Sensitivity of the brain transcriptome to connexin ablation, *Biochim Biophys Acta* **2005**, 1711: 183-196. Review. DOI: 10.1016/j.bbamem.2004.12.002.
9. Iacobas, D.A.; Iacobas, S.; Spray, D.C. Connexin43 and the brain transcriptome of the newborn mice. *Genomics* **2007**, 89(1), 113-123. DOI:10.1016/j.ygeno.2006.09.007.

10. Iacobas, D.A.; Iacobas, S.; Spray, D.C. Connexin-dependent transcellular transcriptomic networks in mouse brain. *Prog Biophys Mol Biol* **2007**, 94(1-2):168-184.
11. Spray, D.C.; Iacobas, D.A. Organizational principles of the connexin-related brain transcriptome. *J Membr Biol* **2007**, 218(1-3):39-47.
12. Wadle S.L.; Augustin, V.; Langer, J.; Jabs, R.; Philippot, C.; Weingarten, D.J. et al. Anisotropic Panglial Coupling Reflects Tonotopic Organization in the Inferior Colliculus. *Front. Cell. Neurosci* **2018**, 12:431. DOI: 10.3389/fncel.2018.00431
13. Papaneophytou, C.; Georgiou, E.; Kleopa, K.A. The role of oligodendrocyte gap junctions in neuroinflammation. *Channels* (Austin) **2019**, 13(1):247-263. DOI: 10.1080/19336950.2019.1631107
14. Vejar, S.; Oyarzún, J.E.; Retamal, M.A.; Ortiz, F.C.; Orellana, J.A. Connexin and Pannexin-Based Channels in Oligodendrocytes: Implications in Brain Health and Disease. *Front Cell Neurosci* **2019**, 13:3. DOI: 10.3389/fncel.2019.00003
15. Lynn, B.D.; Tress, O.; May, D.; Willecke, K., Nagy, J.I. Ablation of connexin30 in transgenic mice alters expression patterns of connexin26 and connexin32 in glial cells and leptomeninges. *Eur J Neurosci* **2011**, 34(11):1783-93. DOI: 10.1111/j.1460-9568.2011.07900.x
16. Guthrie, P.B.; Knappenberger, J.; Segal, M.; Bennett, M.V.; Charles, A.C.; Kater SB. ATP released from astrocytes mediates glial calcium waves. *J Neurosci* **1999**, 19, 520-528. DOI: 10.1523/JNEUROSCI.19-02-00520.1999
17. Ma, J.; Qi, X.; Yang, C.; Pan, R.; Wang, S.; Wu, J. et al. Calhm2 governs astrocytic ATP releasing in the development of depression-like behaviors. *Mol Psychiatry* **2018**, 23(4):883-891. DOI: 10.1038/mp.2017.229
18. Lalo, U.; Bogdanov, A.; Pankratov, Y. Age- and Experience-Related Plasticity of ATP-Mediated Signaling in the Neocortex. *Front Cell Neurosci* **2019**, 13:242. DOI: 10.3389/fncel.2019.00242
19. Iacobas, D.A.; Suadicani, S.O.; Spray, D.C.; Scemes, E. A stochastic 2D model of intercellular Ca2+ wave spread in glia. *Biophys J* **2006**, 90(1): 24-41. DOI:10.1007/s00232-007-9039-7
20. Halassa, M.M.; Florian, C.; Fellin, T.; Munoz, J.R.; Lee, S.Y.; Abel, T. et al. Astrocytic modulation of sleep homeostasis and cognitive consequences of sleep loss. *Neuron* **2009**, 61(2): 213-219. DOI: 10.1016/j.neuron.2008.11.024
21. Schwarz, Y.; Zhao, N.; Kirchhoff, F.; Bruns, D. Astrocytes control synaptic strength by two distinct v-SNARE-dependent release pathways. *Nat Neurosci* **2017**, 20(11):1529-1539. DOI: 10.1038/nn.4647
22. Dong, Y.; Benveniste, E. N. Immune function of astrocytes. *Glia* **2001**, 36, 180–190. DOI: 10.1002/glia.1107
23. Levin, S.G.; Godukhin, O.V. Modulating Effect of Cytokines on Mechanisms of Synaptic Plasticity in the Brain. *Biochemistry* (Mosc) **2017**, 82(3):264-274. DOI: 10.1134/S000629791703004X
24. Santos, C.L.; Bobermin, L.D.; Souza, D.O.; Quincozes-Santos, A. Leptin stimulates the release of pro-inflammatory cytokines in hypothalamic astrocyte cultures from adult and aged rats. *Metab Brain Dis* **2018**, 33(6):2059-2063. DOI: 10.1007/s11011-018-0311-6
25. Kovacs, G.G.; Lee, V.M.; Trojanowski, J.Q. Protein astrogliopathies in human neurodegenerative diseases and aging. *Brain Pathol* **2017**, 27(5):675-690. DOI: 10.1111/bpa.12536
26. Refolo, V.; Stefanova, N. Neuroinflammation and Glial Phenotypic Changes in Alpha-Synucleinopathies. *Front Cell Neurosci* **2019**, 13:263. DOI: 10.3389/fncel.2019.00263
27. Filippini, A.; Gennarelli, M.; Russo, I. α-Synuclein and Glia in Parkinson's Disease: A Beneficial or a Detrimental Duet for the Endo-Lysosomal System? *Cell Mol Neurobiol* **2019**, 39(2):161-168. DOI: 10.1007/s10571-019-00649-9
28. Jimenez-Pascual, A.; Siebzehnrubl, F.A. Fibroblast Growth Factor Receptor Functions in Glioblastoma. *Cells* **2019**, 8(7). DOI: 10.3390/cells8070715
29. Iacobas, S.; Iacobas, D.A. Astrocyte proximity modulates the myelination gene fabric of oligodendrocytes. *Neuron Glia Biology* **2010**, 6(3): 157-169. doi: 10.1017/S1740925X10000220
30. Iacobas, S.; Thomas, N.M.; Iacobas, D.A. Plasticity of the myelination genomic fabric. *Mol Genet Genomics* **2012**, 287:237-246. doi: 10.1007/s00438-012-0673-0.
31. Trotter, J.; Bitter-Suermann, D.; Schachner, M. Differentiation-regulated loss of the polysialylated embryonic form and expression of the different polypeptides of the neural cell adhesion molecule by cultured oligodendrocytes and myelin. *J Neurosci Res* **1989**, 22:369–383. DOI: 10.1002/jnr.490220402
32. Orthmann-Murphy, J.L.; Abrams, C.K.; Scherer, S.S. Gap junctions couple astrocytes and oligodendrocytes. *J Mol Neurosci* **2008**, 35:101–116. DOI: 10.1007/s12031-007-9027-5

33. Iacobas, D.A.; Iacobas, S.; Urban-Maldonado, M.; Scemes, E.; Spray, D.C. Similar transcriptomic alterations in Cx43 knock-down and knock-out astrocytes. *Cell Commun Adhes* **2008**, 15(1), 195-206. . doi:10.1080/15419060802014222.
34. Jung, M.; Krämer, E.; Grzenkowski, M.; Tang, K.; Blakemore, W.; Aguzzi, A. et al. Lines of murine oligodendroglial precursor cells immortalized by an activated neu tyrosine kinase show distinct degrees of interaction with axons in vitro and in vivo. *Eur J Neurosci* **1995**, 7:1245–1265. DOI: 10.1111/j.1460-9568.1995.tb01115.x
35. Lee, P.R.; Cohen, J.E.; Iacobas, D.A.; Iacobas, S.; Fields, R.D. Gene networks activated by pattern-specific generation of action potentials in dorsal root ganglia neurons. *Sci Rep* **2017**, 7:43765. doi:10.1038/srep43765.
36. Iacobas, D.A.; Iacobas, S.; Lee, P.R.; Cohen, J.E.; Fields, R.D. Coordinated Activity of Transcriptional Networks Responding to the Pattern of Action Potential Firing in Neurons. *Genes* **2019**, 10(10), 754. DOI: 10.3390/genes10100754.
37. Kanehisa, M.; Furumichi, M.; Tanabe, M.; Sato, Y. Morishima, K. KEGG: new perspectives on genomes, pathways, diseases and drugs. *Nucleic Acids Res* **2017**, 45, D353-D361. DOI: 10.1093/nar/gkw1092
38. http://www.genome.jp/kegg/
39. Wypych, D.; Pomorski, P. Calcium Signaling in Glioma Cells: The Role of Nucleotide Receptors. *Adv Exp Med Biol* **2020** - Review. PMID 32034709. DOI: 10.1007/978-3-030-30651-9_4
40. Shahcheraghi, S.H.; Tchokonte-Nana, V.; Lotfi, M.; Lotfi, M.; Ghorbani, A.; Sadeghnia, H.R. Wnt/beta-catenin and PI3K/Akt/mtor Signaling Pathways in Glioblastoma: Two main targets for drug design: A Review [published online ahead of print, 2020 Jan 30]. *Curr Pharm Des*. **2020**, 10.2174/1381612826666200131100630. doi:10.2174/1381612826666200131100630
41. Nutma, E.; van Gent, D.; Amor, S.; Peferoen, L.A.N. Astrocyte and Oligodendrocyte Cross-Talk in the Central Nervous System. *Cells* **2020**, 9(3):E600. doi:10.3390/cells9030600.
42. Arneson, D.; Zhang, G.; Ying, Z.; Zhuang, Y.; Byun, H. R.; Ahn, I. S. et al. Single cell molecular alterations reveal target cells and pathways of concussive brain injury. *Nature communications* **2018**, 9(1), 3894. https://doi.org/10.1038/s41467-018-06222-0.
43. Baldassarro, V.A.; Krężel, W.; Fernández, M.; Schuhbaur, B.; Giardino, L.; Calzà, L. The role of nuclear receptors in the differentiation of oligodendrocyte precursor cells derived from fetal and adult neural stem cells. *Stem Cell Res* **2019**, 37:101443. doi:10.1016/j.scr.2019.101443
44. Pusceddu, M.M.; Barboza, M.; Keogh, C.E.; Schneider, M.; Stokes, P.; Sladek, J.A. et al. Nod-like receptors are critical for gut-brain axis signalling in mice. *J Physiol* **2019**, 597(24):5777-5797. doi: 10.1113/JP278640.
45. Iacobas, S.; Neal-Perry, G.; Iacobas, D.A. Analyzing the cytoskeletal transcriptome: sex differences in rat hypothalamus. *Neuromethods* **2013**, 79: 119:133, DOI: 10.1007/978-1-62703-266-7-6
46. Sung, K.; Jimenez-Sanchez, M. Autophagy in Astrocytes and its Implications in Neurodegeneration. *J Mol Biol* **2020**, S0022-2836(20)30023-1. doi:10.1016/j.jmb.2019.12.041
47. Vázquez, A.; Hernández-Oliveras, A.; Santiago-García, J.; Caba, M.; Gonzalez-Lima, F.; Olivo, D. et all. Daily changes in GFAP expression in radial glia of the olfactory bulb in rabbit pups entrained to circadian feeding. *Physiol Behav* **2020**, 217:112824. doi: 10.1016/j.physbeh.2020.112824.
48. Mathew, R.; Huang, J.; Iacobas, S.; Iacobas, D.A. Pulmonary Hypertension Remodels the Genomic Fabrics of Major Functional Pathways. *Genes* **2020**, 11(2), 126; https://doi.org/10.3390/genes11020126.
49. https://www.youtube.com/watch?v=Kc3M5x7125A
50. Iacobas, D.A.; Tuli, N.; Iacobas, S.; Rasamny, J.K.; Moscatello, A.; Geliebter, J.; et al. Gene master regulators of papillary and anaplastic thyroid cancer phenotypes. *Oncotarget* **2018**, 9(2), 2410-2424. doi: 10.18632/oncotarget.23417. PMID: 29416781
51. Iacobas, S.; Ede, N.; Iacobas, D.A. The Gene Master Regulators (GMR) Approach Provides Legitimate Targets for Personalized, Time-Sensitive Cancer Gene Therapy. *Genes* **2019**, 10(8), 560. doi: 10.3390/genes10080560. PMID: 31349573
52. Sarrouilhe, D.; Dejean, C.; Mesnil, M. Connexin43- and Pannexin-Based Channels in Neuroinflammation and Cerebral Neuropathies. *Front Mol Neurosci* **2017**, 10:320. doi: 10.3389/fnmol.2017.00320. PMID: 29066951; PMCID: PMC5641369.
53. Scemes, E.; Veliskova, J. Exciting and Not So Exciting Roles of Pannexins. *Neurosci Lett* **2019**, 695, 25-31. PMCID: PMC5591050 DOI: 10.1016/j.neulet.2017.03.010

54. Spray, D.C.; Iglesias, R.; Shraer, N.; Suadicani, S.O.; Belzer, V.; Hanstein, R. et al. Gap junction mediated signaling between satellite glia and neurons in trigeminal ganglia. *Glia* **2019**, 67(5):791-801. doi: 10.1002/glia.23554. PMID: 30715764; PMCID: PMC6506223.
55. Meng, L.; Zhang, A.; Jin, Y.; Yan, D. Regulation of neuronal axon specification by glia-neuron gap junctions in *C. elegans*. *Elife* **2016**, 5, pii: e19510 (2016). PMID: 27767956 PMCID: PMC5083064 DOI: 10.7554/eLife.19510.
56. Illes, P.; Burnstock, G.; Tang, Y. Astroglia-Derived ATP Modulates CNS Neuronal Circuits. *Trends Neurosci* **2019**, 42(12):885-898. doi: 10.1016/j.tins.2019.09.006.. PMID: 31704181.
57. Trettel, F.; Di Castro, M.A.; Limatola, C. Chemokines: Key Molecules that Orchestrate Communication among Neurons, Microglia and Astrocytes to Preserve Brain Function. *Neuroscience* **2019**, 31:S0306-4522(19)30519-6. doi: 10.1016/j.neuroscience.2019.07.035. PMID: 31376422.
58. Sanna, M.D.; Borgonetti, V.; Galeotti, N. μ Opioid Receptor-Triggered Notch-1 Activation Contributes to Morphine Tolerance: Role of Neuron-Glia Communication. *Mol Neurobiol* **2020**, 57(1):331-345. doi: 10.1007/s12035-019-01706-6. PMID: 31347026.
59. Pascual, M.; Ibáñez, F.; Guerri, C. Exosomes as mediators of neuron-glia communication in neuroinflammation. *Neural Regen Res* **2020**, 15(5):796-801. doi: 10.4103/1673-5374.268893. PMID: 31719239; PMCID: PMC6990780.
60. Iacobas, D.A. The Genomic Fabric Perspective on the Transcriptome between Universal Quantifiers and Personalized Genomic Medicine. *Biological Theory* **2016**, 11(3): 123-137. DOI 10.1007/s13752-016-0245-3
61. Iacobas, D.A.; Iacobas, S.; Werner, P.; Scemes, E.; Spray, D.C. Alteration of transcriptomic networks in adoptive-transfer experimental autoimmune encephalomyelitis. *Front Integr Neurosci* **2007**, 1:10. doi:10.3389/neuro.07/010.2007.
62. Iacobas, D.A.; Iacobas, S. Towards a Personalized Cancer Gene Therapy: A Case of Clear Cell Renal Cell Carcinoma. *Cancer & Oncol Res* **2017**, 5(3): 45-52. DOI:10.13189/cor.2017.050301
63. Frigeri, A.; Iacobas, D.A.; Iacobas, S.; Nicchia, G.P.; Desaphy, J.F.; Camerino, D.C.; et al. Effect of microagravity on brain gene expression in mice. *Exp Brain Res* **2008**, 191(3): 289-300. doi: 10.1007/s00221-008-1523-5.
64. Iacobas, D.A.; Fan, C.; Iacobas, S.; Spray, D.C.; Haddad, G.G. Transcriptomic changes in developing kidney exposed to chronic hypoxia. *Biochem Biophys Res Comm* **2006**, 349(1), 329-338. DOI:10.1016/j.bbrc.2006.08.056.
65. Iacobas, D.A.; Fan, C.; Iacobas, S.; Haddad, G.G. Integrated transcriptomic response to cardiac chronic hypoxia: translation regulators and response to stress in cell survival. *Funct Integr Genomics* **2008**, 8(3):265-75. doi: 10.1007/s10142-008-0082-y.
66. Iacobas, D.A.; Iacobas, S.; Haddad, G.G. Heart rhythm genomic fabric in hypoxia. *Biochem Biophys Res Commun* **2010**, 391(4):1769-1774. doi: 10.1016/j.bbrc.2009.12.151. PMCID:PMC2849310.
67. Kaufman, R.J.; Scheuner, D.; Schröder, M.; Shen, X.; Lee, K.; Liu, C.Y. et al. The unfolded protein response in nutrient sensing and differentiation. *Nat Rev Mol Cell Biol* **2002**, 3(6):411-21. doi: 10.1038/nrm829. PMID: 12042763
68. Ariyasu, D.; Yoshida, H.; Hasegawa, Y. Endoplasmic Reticulum (ER) Stress and Endocrine Disorders. *Int J Mol Sci* **2017**, 18(2). pii: E382. PMID: 28208663 PMCID: PMC5343917 DOI: 10.3390/ijms18020382
69. Guizzetti, M.; Kavanagh, T.J.; Costa, L.G. Measurements of astrocyte proliferation. *Methods Mol Biol* **2011**, 758:349-59. PMID: 21815078 DOI: 10.1007/978-1-61779-170-3_24
70. Knight, V.B.; Serrano, E.E. Post-Translational Tubulin Modifications in Human Astrocyte Cultures. *Neurochem Res* **2017**, 42(9):2566-2576. PMID: 28512712 PMCID: PMC5710013 DOI: 10.1007/s11064-017-2290-0
71. Liceras-Boillos, P.; García-Navas, R.; Ginel-Picardo, A.; Anta, B.; Pérez-Andrés, M.; Lillo, C. et al. Sos1 disruption impairs cellular proliferation and viability through an increase in mitochondrial oxidative stress in primary MEFs. *Oncogene* **2016**, 35(50):6389-6402. PMID: 27157612 DOI: 10.1038/onc.2016.169
72. Patel, S.A.; Simon, M.C. Functional analysis of the Cdk7.cyclin H.Mat1 complex in mouse embryonic stem cells and embryos. *J Biol Chem* **2010**, 285(20):15587-98. PMID: 20231280 PMCID: PMC2865308 DOI: 10.1074/jbc.M109.081687
73. Rajaraman, P.; Wang, S.S.; Rothman, N.; Brown, M.M.; Black, P.M.; Fine, H.A. et al. Polymorphisms in apoptosis and cell cycle control genes and risk of brain tumors in adults. *Cancer Epidemiol Biomarkers Prev* **2007**, 16(8):1655-61. doi: 10.1158/1055-9965.EPI-07-0314. PMID: 17684142.

74. Basu, R.; Sarma, J.D. Connexin 43/47 channels are important for astrocyte/ oligodendrocyte cross-talk in myelination and demyelination. *J Biosci* **2018**, 43(5):1055-1068. PMID: 30541963.
75. Nagy, J.I.; Ionescu, A.V.; Lynn, B.D.; Rash, J.E. Coupling of astrocyte connexins Cx26, Cx30, Cx43 to oligodendrocyte Cx29, Cx32, Cx47: Implications from normal and connexin32 knockout mice. *Glia* **2003**, 44(3):205-18. doi: 10.1002/glia.10278. PMID: 14603462; PMCID: PMC1852517.
76. Allen, N.J.; Eroglu, C. Cell Biology of Astrocyte-Synapse Interactions. *Neuron* **2017**, 96(3):697-708. doi: 10.1016/j.neuron.2017.09.056. PMID: 29096081; PMCID: PMC5687890.
77. Farhy-Tselnicker, I.; Allen, N.J. Astrocytes, neurons, synapses: a tripartite view on cortical circuit development. *Neural Dev* **2018**, 13(1):7. doi: 10.1186/s13064-018-0104-y. PMID: 29712572; PMCID: PMC5928581.
78. Tso, C.F.; Simon, T.; Greenlaw, A.C.; Puri, T.; Mieda, M.; Herzog, E.D. Astrocytes Regulate Daily Rhythms in the Suprachiasmatic Nucleus and Behavior. *Curr Biol* **2017**, 27(7):1055-1061. doi: 10.1016/j.cub.2017.02.037. PMID: 28343966; PMCID: PMC5380592.
79. Brancaccio, M.; Patton, A.P.; Chesham, J.E.; Maywood, E.S.; Hastings, M.H. Astrocytes Control Circadian Timekeeping in the Suprachiasmatic Nucleus via Glutamatergic Signaling. *Neuron* **2017**, 93(6):1420-1435.e5. doi: 10.1016/j.neuron.2017.02.030. PMID: 28285822; PMCID: PMC5376383.
80. Ali, A.A.H.; Stahr, A.; Ingenwerth, M.; Theis, M.; Steinhäuser, C.; von Gall, C. Connexin30 and Connexin43 show a time-of-day dependent expression in the mouse suprachiasmatic nucleus and modulate rhythmic locomotor activity in the context of chronodisruption. *Cell Commun Signal* **2019**, 17(1):61. doi: 10.1186/s12964-019-0370-2. PMID: 31186021; PMCID: PMC6560876.
81. Busino, L.; Bassermann, F.; Maiolica, A.; Lee, C.; Nolan, P.M.; Godinho, S.I.H.; et al. SCFFbxl3 controls the oscillation of the circadian clock by directing the degradation of cryptochrome proteins. *Science* **2007**, 316: 900–904. PMID: 17463251 DOI: 10.1126/science.1141194.
82. Brancaccio, M.; Edwards, M.D.; Patton, A.P.; Smyllie, N.J.; Chesham, J.E.; Maywood, E.S. et al. Cell-autonomous clock of astrocytes drives circadian behavior in mammals. *Science* **2019**, 363.6423: 187-192. doi: 10.1126/science.aat4104. PMID: 30630934
83. Clasadonte, J.; Scemes, E.; Wang, Z.; Boison, D.; Haydon P.G. Connexin 43-mediated astroglial metabolic networks contribute to the regulation of the sleep-wake cycle. *Neuron* **2017**, 95.6: 1365-1380. PMID: 28867552 PMCID: PMC5617118 DOI: 10.1016/j.neuron.2017.08.022
84. Cirelli, C.; Tononi, G. Gene expression in the brain across the sleep–waking cycle. *Brain research* **2000**, 885.2: 303-321. doi: 10.1016/s0006-8993(00)03008-0. PMID: 11102586.
85. Morte, B.; Gil-Ibáñez, P.; Bernal, J. Regulation of Gene Expression by Thyroid Hormone in Primary Astrocytes: Factors Influencing the Genomic Response. *Endocrinology* **2018**, 159(5):2083-2092. doi: 10.1210/en.2017-03084. PMID: 29617759.
86. Almazan, G.; Honegger, P.; Matthieu, J.M. Triiodothyronine stimulation of oligodendroglial differentiation and myelination. A developmental study. *Dev Neurosci* **1985**, 7(1):45-54. doi: 10.1159/000112275. PMID: 2411494.
87. Shanker, G.; Campagnoni, A.T.; Pieringer, R.A. Investigations on myelinogenesis in vitro: developmental expression of myelin basic protein mRNA and its regulation by thyroid hormone in primary cerebral cell cultures from embryonic mice. *J Neurosci Res* **1987**, 17(3):220-4. doi: 10.1002/jnr.490170304. PMID: 2439700.
88. Mendes, A.I.; Matos, P.; Moniz, S.; Jordan, P. Protein kinase WNK1 promotes cell surface expression of glucose transporter GLUT1 by regulating a Tre-2/USP6-BUB2-Cdc16 domain family member 4 (TBC1D4)-Rab8A complex. *J Biol Chem* **2010**, 285(50):39117-26. doi: 10.1074/jbc.M110.159418. PMID: 20937822; PMCID: PMC2998075.